Design of synthetic extracellular matrices for probing breast cancer cell growth using robust cyctocompatible nucleophilic thiol-yne addition chemistry

Macdougall, Laura J.; Wiley, Katherine L.; Kloxin, April M.; Dove, Andrew

DOI:
10.1016/j.biomaterials.2018.04.046

Document Version
Peer reviewed version

Citation for published version (Harvard):
Macdougall, LJ, Wiley, KL, Kloxin, AM & Dove, A 2018, 'Design of synthetic extracellular matrices for probing breast cancer cell growth using robust cyctocompatible nucleophilic thiol-yne addition chemistry', *Biomaterials*. https://doi.org/10.1016/j.biomaterials.2018.04.046

Accepted Manuscript

Design of synthetic extracellular matrices for probing breast cancer cell growth using robust cyctocompatible nucleophilic thiol-yne addition chemistry

Laura J. Macdougall, Katherine L. Wiley, April M. Kloxin, Andrew P. Dove

PII: S0142-9612(18)30310-7

DOI: 10.1016/j.biomaterials.2018.04.046

Reference: JBMT 18632

To appear in: *Biomaterials*

Received Date: 29 January 2018

Revised Date: 27 March 2018

Accepted Date: 23 April 2018

Please cite this article as: Macdougall LJ, Wiley KL, Kloxin AM, Dove AP, Design of synthetic extracellular matrices for probing breast cancer cell growth using robust cyctocompatible nucleophilic thiol-yne addition chemistry, *Biomaterials* (2018), doi: 10.1016/j.biomaterials.2018.04.046.

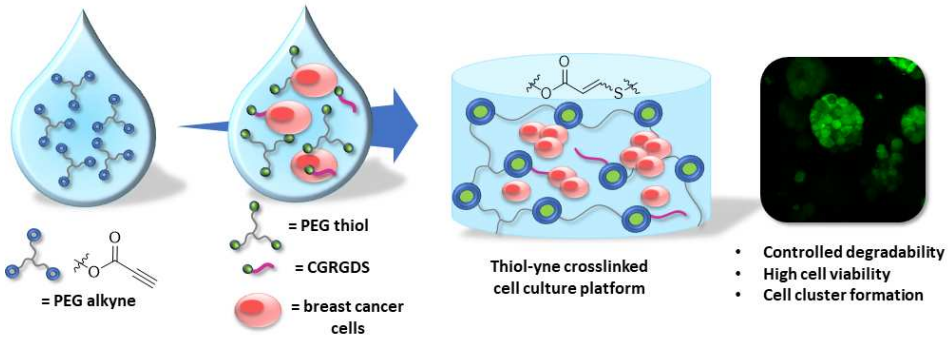

Design of Synthetic Extracellular Matrices for Probing Breast Cancer Cell Growth Using Robust Cyctocompatible Nucleophilic Thiol-yne Addition Chemistry

Laura J. Macdougall, [a, 1] *Katherine L. Wiley,* [c, 1] *April M. Kloxin* [c, d*] *and Andrew P. Dove* [a,b*]

[a] Department of Chemistry, University of Warwick, Gibbet Hill Road, Coventry, CV4 7AL, UK

[b] School of Chemistry, University of Birmingham, Edgbaston, Birmingham, B15 2TT, UK

[c] Department of Chemical and Biomolecular Engineering, University of Delaware, Newark, DE 19716, USA

[d] Department of Materials Science and Engineering, University of Delaware, Newark, DE 19716, USA

[1] *Laura J. Macdougall and Katherine L. Wiley contributed equally to this work*

KEYWORDS

Poly (ethylene glycol), Nucleophilic thiol-yne, Hydrogels, Breast cancer, 3D culture, Synthetic extracellular matrices

ABSTRACT

Controlled, three-dimensional (3D) cell culture systems are of growing interest for both tissue regeneration and disease, including cancer, enabling hypothesis testing about the effects of microenvironment cues on a variety of cellular processes, including aspects of disease progression. In this work, we encapsulate and culture in three dimensions different cancer cell lines in a synthetic extracellular matrix (ECM), using mild and efficient chemistry. Specifically, harnessing the nucleophilic addition of thiols to activated alkynes, we have created hydrogel-based materials with multifunctional poly(ethylene glycol) (PEG) and select biomimetic peptides. These materials have definable, controlled mechanical properties (*G'*= 4-10 kPa) and enable facile incorporation of pendant peptides for cell adhesion, relevant for mimicking soft tissues, where polymer architecture allows tuning of matrix degradation. These matrices rapidly formed in the presence of sensitive breast cancer cells (MCF-7) for successful encapsulation with high cell viability, greatly improved relative to that observed with the more widely used radically-initiated thiol-ene crosslinking chemistry. Furthermore, controlled matrix degradation by both bulk and local mechanisms, ester hydrolysis of the polymer network and cell-driven enzymatic hydrolysis of cell-degradable peptide, allowed cell proliferation and the formation of cell clusters within these thiol-yne hydrogels. These studies demonstrate the importance of chemistry in ECM mimics and the potential thiol-yne chemistry has as a crosslinking reaction for the encapsulation and culture of cells, including those sensitive to radical crosslinking pathways.

1. INTRODUCTION

Three-dimensional (3D) culture systems are of continued and growing interest for studies of both tissue regeneration and disease, including cancer.[1-4] For example, in the study of breast cancer, seminal works have demonstrated the relevance of 3D culture for *in vitro* studies to recapture *in vivo* breast cancer phenotypes and the importance of extracellular matrix (ECM) signaling in cancer cell growth and metastasis.[5-7] Traditionally, such 3D culture studies often have utilized protein matrices harvested from tissues, such as basement membrane extract (or Matrigel)[8] and collagen I.[9, 10] Owing to the complex nature of cancer progression and many other maladies, design and deployment of well-defined synthetic mimics of the extracellular matrix provides opportunities for hypothesis testing about the effects of specific microenvironment cues, as well as systems for the screening of drug candidates, without the batch-to-batch variation of harvested materials.[11, 12] Synthetic biomaterials, such as hydrogels, have proven to be useful tools for mimicking key aspects of the mechanical and biochemical properties of the ECM in a variety cell culture applications.[13-15] In recent years, there has been heightened interest in synthetic PEG hydrogel-based ECM mimics as a consequence of their controlled mechanical properties and ability to include a wide range of biochemical cues.[16] In particular, seminal studies have demonstrated how matrix degradability and integrin-binding can be key properties for a many cellular processes, from cell adhesion and proliferation to motility and differentiation,[17-19] where a variety of chemistries with different degrees of biocompatibility and property control have been used. These studies highlight the opportunity that such well-defined materials provide for 3D cell culture and the need for more robust and cytocompatible chemistries for the generation and modification of these systems in the presence of cells.

In the study of breast cancer, such well-defined materials have provided unique tools for multidimensional culture studies and insights into key cell-matrix interactions in different

aspects of disease progression.[16, 20, 21] For example, the use of high-throughput methods of PEG hydrogel components has enabled better predictions of *in vivo* cancer cell behaviors while allowing us to refine the specific characteristics of different cancer microenvironments that influence cell behavior and cancer progression.[22-25] Further to this, the capability to encapsulate breast cancer cells into PEG hydrogel microspheres for high throughput analysis has been demonstrated, an approach which provides alternatives to screening assays typically performed on tissue culture treated plastic with the potential for increased physiological relevance.[26] Additionally, several groups have utilized PEG hydrogels to probe the influence of matrix stiffness on breast cancer progression.[27, 28] Combined with recent advances in characterization of cytokine secretion from 3D matrices, it is understood that the role of matrix interactions on the phenotypic properties of cancer cells is incredibly influential.[16, 20, 29, 30] These observations have confirmed that material properties are fundamental to furthering our understanding of breast cancer cell response to different microenvironments and the ability to fine-tune the mechanical and biochemical properties of their culture environment.[31-36] Building upon these studies, opportunities remain in the establishment of new robust and accessible chemistries for the formation and modulation of matrix properties for the 3D culture of breast cancer cells and related niche cells. Of particular interest are chemistry-based approaches for the formation of hydrogels in the presence of cells sensitive to chemical stimuli (*e.g.*, free radicals or catalysts).[37, 38] Further, the formation of hydrogels that do not swell, and hence retain their mechanical properties for longer, would provide opportunities for the seamless integration of such well-defined materials systems within microfluidic devices for more complex studies of cell-microenvironment interactions (*e.g.*, under fluid flow and in co-culture).[39]

The judicious choice of the crosslinking chemistry used for the formation of synthetic matrices is important for the facile encapsulation of a range of cell types and their culture

over time.[40] Bioorthogonal click chemistries (*e.g.*, copper catalyzed azide-alkyne cycloaddition (CuAAC), strain promoted azide-alkyne cycloaddition (SPAAC), thiol-ene, oxime, inverse electron demand Diels-Alder and thiol-yne reactions) enable the synthesis of hydrogels under physiological conditions (pH 7.4 at 37 °C).[41-43] These chemistries have been widely used with a range of different synthetic and natural polymers[44, 45] to form hydrogels that are not only biocompatible but can also be tuned to certain mechanical properties depending on the application required.[46-48] Furthermore, these materials are incredibly versatile: the networks can be post modified with a wide range of biologically relevant molecules (*e.g.*, binding peptides) to increase the biocompatibility of these materials and to mimic specific ECM compositions,[44, 49] and their mechanical properties (*e.g.*, stiffness) can be tuned to mimic the naturally occurring matrix.[50, 51] In this respect, thiol-ene chemistry stands out amongst these, owing to the ease of *i)* peptide incorporation within networks by inclusion of cysteines within sequences of interest, including integrin-binding ligands and cell-degradable crosslinks, and *ii)* control of matrix modulus with functional group stoichiometry and monomer concentration during hydrogel formation.[42, 52] However, these existing chemistries are not without drawbacks. For example, the cytotoxicity of copper catalyzed click chemistry motivated the move to SPAAC chemistry[53] for 3D culture applications, yet the synthesis of SPAAC precursors remains challenging and commercially-available products costly. Although radical initiated thiol-ene chemistry has been used successfully for a broad range of cell culture applications, the sensitivity of particular cells to free radicals and the reactive oxygen species they may generate could hinder their use with some cellular systems.[54] Consequently, chemical approaches for the creation of 3D culture systems are still needed that not only provide the click chemistry trademark of rapid gel formation at physiological conditions but also are free of catalyst or initiator using accessible and easily synthesized hydrogel precursors.

In this work, we aimed to provide a complementary approach by establishing the utility and versatility of nucleophilic thiol-yne addition chemistry for encapsulation and culture of cells within hydrogels that undergo both programmed and cell-driven degradation, particularly for sensitive breast cancer cells. The nucleophilic thiol-yne addition is a reaction in which the *in situ* generation of a thiolate anion by mild base (pH 7.4) allows for nucleophilic attack on an activated alkyne such as a propiolate ester, thus allowing the formation of robust cytocompatible hydrogel materials in an efficient manner without the need for an external catalyst (*e.g.*, light or a metal catalyst), free radicals, or any external stimulus.[55-57] The precursors are easy to incorporate into the polymer precursors and the resultant hydrogels require no additional purification steps. Overall the nucleophilic thiol-yne reaction is unparalleled in its simplicity and therefore an ideal reaction for the synthesis of hydrogels under physiological conditions. Previously, we have shown that this crosslinking chemistry can be used to form biocompatible hydrogel materials that are tunable and robust,[58] and through careful consideration of architecture, can be nonswelling.[59] Herein, we have developed a nucleophilic thiol-yne PEG hydrogel platform to act as an ECM mimic for the encapsulation and 3D culture of a range of different breast cancer cell lines: MDA-MB-231, highly aggressive, invasive triple negative breast cancer cells; T47D, estrogen receptor positive (ER+) breast cancer cells; and most notably MCF-7, ER+ breast cancer cells that are used extensively as a model ER+ breast cancer cell line.[60] In this work, the nucleophilic thiol-yne chemistry uniquely has been exploited to demonstrate the ability of this platform to create materials that mimic the mechanical properties of soft tissues, enable the facile incorporation of bioactive peptides for promoting cell adhesion, and allow fine-tuning local and bulk network degradation. This work showcases the potential for thiol-yne PEG-based hydrogels to be used for the culture of breast cancer cells for probing cell-microenvironment

interactions in a matrix with highly controlled mechanical and biochemical properties and of relevance for future studies with other sensitive cell types.

2. MATERIALS AND METHODS

2.1 Materials

Unless otherwise noted, all reagents were purchased from Sigma-Aldrich or Fisher Scientific and used without purification.

2.2 Instrumental methods

^{1}H NMR spectra were recorded on a Bruker DPX-400 spectrometer at 293 K. Chemical shifts are reported as δ in parts per million (ppm) and referenced to the chemical shift of the residual solvent resonances ($CDCl_3$: ^{1}H δ = 7.26 ppm; $(CD_3)_2CO$: ^{1}H δ = 2.05 ppm).

Size exclusion chromatography (SEC) was used to determine the molar masses and molar mass distributions (dispersities, $Đ_M$) of the synthesized polymers. SEC conducted in chloroform ($CHCl_3$) (0.5% NEt_3) used a Varian PL-SEC 50 system equipped with 2 × PLgel 5 μM MIXED-D columns in series and a differential refractive index (RI) detector at a flow rate 1.0 mL min^{-1}. The system was calibrated against a Varian Polymer Laboratories Easi-Vial poly(styrene) (PS) standard and analyzed by the software package Cirrus v3.3.

SEC conducted in *N*,*N*-dimethyl formamide (DMF) (5 mM NH_4BF_4) used a Varian PL-SEC 50 system equipped with 2 × PLgel 5 μM MIXED-C + guard columns in series and a differential refractive index (RI) detector at a flow rate of 1.0 mL min^{-1}. The systems were calibrated against Varian Polymer Laboratories Easi-Vial linear poly(methyl methacrylate) (PMMA) standards and analyzed by the software package Cirrus v3.3.

Rheological testing was carried out using an Anton Parr MCR 302 rheometer equipped with parallel plate configuration with a diameter of 50 mm. A Peltier system was used to maintain the temperature at 20 °C throughout the study. Data was analyzed using RheoCompass software.

Compression testing was carried out using single column universal materials testing machine M100-1CT Testometric with a load cell of 50 N. Data was analyzed using Wintest analysis software.

2.3 Cell culture and maintenance

The MDA-MB-231, T47D, and MCF-7 cell lines were used in this study. MDA-MB-231 and T47D cell lines were maintained in Dulbecco's Modified Eagle Medium (DMEM; Corning 10-013-CV) supplemented with 10 vol% fetal bovine serum (FBS), 1 vol% Glutamax and 1 vol% penicillin/streptomycin (PS). The MCF-7 cell line was maintained in DMEM supplemented with 5 vol% FBS and 1 vol% PS.

2.4 Synthesis of gel precursors

3-arm alkyne functionalized PEG (1 kg mol^{-1}). In a typical esterification, as previously published,[59] glycerol ethoxylate (molar mass 1.0 kg mol^{-1}, 10 g, 10 mmol) was esterified with propiolic acid (4.2 g, 60 mmol) to collect the product as a light yellow oil (Yield 8.1 g, 70%). ^{1}H NMR ($(CD_3)_2CO$, 400 MHz): δ 4.32-4.34 (t, $^3J_{HH}$ = 8 Hz, -C*H*$_2$OCO-), 3.89 (s, -C*H*≡CC(O)O-), 3.71-3.74 (m, -OC*H*$_2$C*H*$_2$O-), 3.58 (s, -CC*H*$_2$O); ^{1}H NMR spectroscopy indicated *ca.* 92% conversion of the hydroxyl group to propiolate group. SEC (DMF): M_n = 3.3 kg mol^{-1} ($Đ_M$ = 1.04).

3-arm thiol functionalized PEG (1 kg mol^{-1}). In a typical esterification as stated in the above procedure, glycerol ethoxylate (molar mass 1.0 kg mol^{-1}, 10 g, 10 mmol) was esterified using 3-mercaptopropionic acid (4.2 g, 60 mmol). (Yield 9.4 g, 74%). ^{1}H NMR ($CDCl_3$, 400 MHz): δ 4.20-4.22 (t, $^3J_{HH}$ = 8, -C*H*$_2$OCO-), 3.58 (m, -OC*H*$_2$C*H*$_2$O-), 2.69-2.74 (q, $^3J_{HH}$ = 12, -OCCH$_2$C*H*$_2$SH), 2.61-2.64 (t, $^3J_{HH}$ =12, -OCC*H*$_2$CH$_2$SH), 1.61-1.66 (t, $^3J_{HH}$ = 20, -S*H*), ^{1}H

NMR spectroscopy indicated *ca.* >99% conversion of the hydroxyl group to mercaptopropionate group. SEC (DMF): M_n = 1 .6 kg mol^{-1} ($Đ_M$ = 1.08).

2-arm thiol functionalized PEG (2 kg mol^{-1}). In a typical esterification, as stated in the above procedure, 2-arm PEG-OH (10 g, 10 mmol) was esterified with 3-mercaptopropionic acid (2 equivalents per arm/ 0.5 kg mol^{-1}) to collect the product as a white solid (Yield 9.2 g, 85%). ^{1}H NMR ($CDCl_3$, 400 MHz): δ 4.26-4.28 (t, $^3J_{HH}$ = 8, -C*H*$_2$OCO-), 3.65 (m, -OC*H*$_2$C*H*$_2$O-), 2.75-2.80 (q, $^3J_{HH}$ = 12, -OCCH$_2$C*H*$_2$SH), 2.67-2.70 (t, $^3J_{HH}$ =12, -OC*H*$_2$CH$_2$SH), 1.67-1.69 (t, $^3J_{HH}$ = 8, -S*H*), ^{1}H NMR spectroscopy indicated *ca.* >99% conversion of the hydroxyl group to mercaptopropionate group. SEC ($CHCl_3$): M_n = 2.7 kg.mol^{-1} ($Đ_M$ = 1.26).

Thiol functionalized peptide synthesis. Both the pendant adhesion peptide (**C**GRGDS) and MMP-degradable crosslinking peptide (G**C**RDVPMS↓MRGGDR**C**G) were synthesized using standard solid phase peptide synthesis (SPPS) on MBHA rink amide resin (Novabiochem) on a peptide synthesizer (Protein Technologies PS3) using Fmoc-protected amino acids (ChemPep), deprotected with 20% piperidine in *N*,*N*-dimethylformamide (DMF) and activated with *O*-(Benzotriazole-1-yl)-*N*,*N*,*N*',*N*'-tetramethyluronium hexafluorophosphate (HBTU) at 4 × excess. Peptide was cleaved from resin with a cleavage solution containing 95% v/v trifluoroacetic acid (TFA), 2.5 v/v triisopropylsilane (TIPS), 2.5% v/v water, and 5% w/v dithiothreitol (DTT) to prevent disulfide formation. The cleavage solution containing the peptide product was precipitated into cold ether, then pelleted by centrifugation (4400 rpm, 4 °C, 5 min). Decanted for a total of three ether washes and then dried overnight. Peptides were purified by high-performance liquid chromatography (HPLC; XBridge BEH C18 OBD 5 μm column; Waters, Milford, MA) with a linear water-acetonitrile gradient and molecular weight was verified by electrospray ionization mass

spectrometry (ESI-MS; Waters Acquity H-Class UPLC/SQD2, Waters, Milford, MA; ESI Figure S1).

Thiol-ene gel precursors. Thiol-ene gel precursors, including $PEG_{20k}(SH)_4$, macromer, alloc-functionalized peptides (K(alloc)GWGRGDS and KK(alloc)GGPQIWGQGK(alloc)K), and lithium acylphosphinate (LAP) were synthesized according to the previously published protocol.[61, 62]

2.5 Hydrogel fabrication

Thiol-yne hydrogel synthesis. A 1:1 molar ratio of alkyne group to thiol group was used for all gelations by thiol-yne chemistry unless stated otherwise and the precursor content was kept at 10 wt%. In a typical procedure for making a thiol-yne PEG gel, $PEG_{1k}(SH)_3$ (7.9 mg, 6.23×10^{-6} mmol) was dissolved in 75 μL Dulbecco's phosphate-buffered saline (PBS, pH 7.4) solution or DMEM. A separate solution of $PEG_{1k}(C{\equiv}CH)_3$ (7.2 mg, 6.23×10^{-6} mmol) in 75 μL PBS (pH 7.4) or DMEM. The two solutions were mixed together on a vortex mixer for 5 s. 20 μL of hydrogel solution was then pipetted into a 1 mL syringe mold and left to cure.

Validation of pendant peptide incorporation. Standard solutions of thiol-functional fluorescent peptide in PBS were prepared at various concentrations (0.1, 0.5, 1, 2, 3, 4 mM). Thiol-yne hydrogels were formed according to the above protocol and soaked in the standard fluorescent peptide solutions overnight. Thiol-yne hydrogels were synthesized with 5 mM thiol-functionalized fluorescent peptide and swollen in PBS or phenol red free media overnight. Images of fluorescence were captured with a LSM 810 confocal microscope (Zeiss), with a 488 nm laser. Fluorescence of each image was quantified in ImageJ. Fluorescence of standards were graphed by concentration and fit linearly. The linear fit

equation was used to determine the concentration of fluorescent peptide covalently incorporated into the gels.

Thiol-ene hydrogel synthesis. A solution of 10 wt% $PEG_{20k}(SH)_4$, a stoichiometric amount of alloc-functionalized crosslinker (KK(alloc)GGPQIWGQGK(alloc)K) and 2 mM of alloc-functionalized fibronectin mimetic peptide (K(alloc)GWGRGDS) and 2 mM LAP were combined in DMEM. 20 μL of the hydrogel solution was then pipetted into a 1 mL syringe mold and polymerized by exposure to 365 nm light (10 mW cm^{-2}) for 1 min.

2.6 Mechanical Characterization

Rheological Testing. All rheology was performed on an Anton Parr MCR 302 rheometer fitted with a parallel plate configuration (diameter of 8 mm) at 21 °C. In a typical rheological test for gelation kinetics, $PEG_{1k}(SH)_3$ (5.5 mg, 4.33×10^{-3} mmol) and $PEG_{1k}(C{\equiv}CH)_3$ (5.0 mg, 4.33×10^{-3} mmol) were dissolved in separate solutions of 50 μL DMEM. The two solutions were mixed together and injected on to the lower plate, at 21 °C. The upper plate was lowered immediately to a plate separation of 2 mm, and the measurement was started. A frequency of 5 Hz and a strain of 5% was applied to minimize interference with the gelation process and keep the measurement within the linear viscoelastic region. The normal force was also kept constant at 0 N. The gelation kinetics was characterized by the evolution of storage moduli (*G*') and loss moduli (*G*") as a function of time. The gel point was determined by the cross-over between the *G*' and *G*". A point was recorded each second until the *G*' and *G*" plateaued. The amplitude and frequency sweeps were carried out on the gel formed from this experiment. The amplitude sweep applied a constant frequency of 10 rad s^{-1}, and the strain was ramped logarithmically from 0.01% to 100%. The normal force was kept constant at 0 N and 6 points were recorded for each decade. All measurements were repeated in triplicate and representative charts are shown. The frequency sweep applied a constant strain

of 0.5%, and the angular frequency was ramped logarithmically from 100 rad s^{-1} to 0.1 rad s^{-1}. The normal force was kept constant at 0 N throughout the test, and 5 points were taken each decade. All measurements were repeated in triplicate, and the average storage and loss moduli were calculated from the frequency sweep experiments at 10 rad s^{-1} and 0.5% strain.

Young's Modulus calculations. Young's Moduli were calculated from the average rheological *G'* and *G"* values using the equation:[63]

$$E = 2G(1 + \vartheta) \text{ and } G = \sqrt{G'^2 + G''^2}$$

Where E = Young's Modulus, ϑ = 0.5 (Poisson's ratio for hydrogel materials),[49] G= shear modulus, G'= shear storage modulus and G''= shear loss modulus.

Uniaxial compressive tests. All uniaxial compressive testing was performed on a M100-1CT Testometric fitted with a load cell of 50 N. Hydrogel samples were prepared with a 2 mL syringe to give a cylindrical shape with a diameter of 9 mm and thickness of 4 mm. Samples were left to cure for 1 h after forming, to ensure the crosslinking reaction was complete before being tested. A preload force of 0.1 N was set, and each test was carried out at a compression velocity of 5 mm min^{-1}. Each hydrogel was subject to strain until failure in order to determine the ultimate compressive stress and strain. All compression tests were repeated 10 times, and an average of the data was taken to find the ultimate compressive stress and strain. Data was analyzed using Wintest analysis software.

2.7 Biocompatibility studies and 3D cell encapsulation

Cell encapsulation in 3D thiol-yne and radically-initiated thiol-ene hydrogels. Trypsin (0.25% Trypsin / 0.1% EDTA) was added to cells, and incubated at 37 °C, until all the cells detached (~3 mins), the solution was then quenched with culture medium. Cells were centrifuged (1,000 rpm, 5 mins) and resuspended in serum-free DMEM. Cells were mixed

with hydrogel precursor solution, and polymerizations proceeded as noted for hydrogel fabrication. For thiol-yne chemistry, it is critical that cells be mixed with the thiol-containing gel precursor first to limit exposure to any potential hydrolysis products of PEG alkyne before polymerization.

Cell metabolic activity (two-dimensional (2D) culture). For 2D cell culture, cell metabolic activity was assessed using the CellTiter 96 assay, a colorimetric assay which includes a tetrazolium compound and an electron coupling reagent, phenazine ethosulfate. On day -1, cells were seeded in a 96-well plate (n=3) at a concentration of 15,000 cells cm^{-2}. On day 0, cells were exposed to the desired treatments. For each treatment, 50 μL of solution was added to each well and incubated at room temperature for 15 mins. The only treatment that was not incubated for 15 mins was the radically-initiated thiol-ene treatment. Treatments included: Medium (control), PBS solution, thiol-ene, PEG alkyne, cysteine only, and thiol-yne. The thiol-ene treatment mimicked thiol-ene gelation conditions and included a 10 wt% solution of $PEG_{3.4k}(SH)_2$, 2-allyl functionalized peptide, and LAP in PBS, which was added to wells, then exposed to long wavelength UV light (365 nm, 10 mW cm^{-2}) for 1 min. The PEG alkyne treatment included a solution of $PEG_{1k}(C{\equiv}CH)_3$ in PBS (concentration equivalent for making 10 wt% gels). The cysteine only treatment was a solution of cysteine in PBS (concentration equivalent to the number of thiol groups present in 10 wt% thiol-yne PEG gel formation). The thiol-yne treatment mimicked thiol-yne gelation conditions by incorporating concentrations of $PEG_{1k}(C{\equiv}CH)_3$ and thiol (cysteine) required to form a 10 wt% thiol-yne PEG hydrogel in PBS. Once the treatment was removed, 100 μL of fresh culture media were added to each well. The media were exchanged after 1 h. Metabolic activity of the cells was assessed on day 1 and day 3. For day 3 samples, the 100 μL of media were changed on day 2. The metabolic activity was assessed according to the manufacturer's

instructions. Briefly, 20 μL of CellTiter 96 solution was added to each well; the plates were incubated for 4 h; and then the absorbance was measured on a plate reader at 490 nm.

Cell metabolic activity (3D culture). For 3D cell culture, cell metabolic activity was assessed using the alamarBlue assay. On day 0, cells were encapsulated in gels (n=4) and placed in 48-well plates with 500 μL of media. Metabolic activity was assessed on day 1, day 3, and day 7. Metabolic activity of the cells was assessed according to the manufacture's instructions. Briefly, alamarBlue reagent was diluted 1:10 in phenol red free media, then media were removed from each well, and 500 μL of diluted alamarBlue solution added to each well. Well plates were incubated for 4 h, then the fluorescence was measured on a plate reader (Ex = 560, Em = 590). Media were replaced on the gels, since the same gels were measured at each time point.

Cell viability assay (3D culture). Cell viability for 3D cell culture was assessed using a Live/Dead Assay Kit, including calcein AM and ethidium homodimer. Working solution was prepared by adding 0.5 μL of calcein AM and 2 μL of ethidium homodimer to 1 mL of PBS. On day 0, cells were encapsulated in gels (n=3) and placed in 48-well plates with 500 μL of media. Cell viability was assessed on day 1, day 3, day 7, and day 10. On the day of assay, media were removed, and 500 μL of working solution was added. Thiol-yne gels were incubated for 30 mins and thiol-ene gels were incubated for 10 mins, to account for differences in diffusion due to variation in matrix densities between the two systems. Fluorescence imaging in three-dimensions was captured with a LSM 810 confocal microscope (Zeiss). Staining for live cells (Calcein, Ex. = 495 nm, Em. = 515 nm) was excited with a 488 nm laser, while staining for dead cells (Ethidium homodimer, Ex = 528 nm, Em = 617 nm) was excited with a 514 nm laser. Z-stacks with an average thickness of

200 μm were collected from three different x-y zones of each sample and orthogonal projections were obtained from each Z-stack. Images were processed using ImageJ software.

Analysis of cell cluster diameter was carried out using confocal microscopy and images processed using Volocity (Perkin Elmer). All compositions were formed in serum free media (2,500 cells μL^{-1}). Cell clusters were stained with calcein and images were taken in 200 μm stacks (interval = 5.7 μm) by confocal microscopy (LSM 810 confocal microscope; Zeiss). Images were then processed using Volocity (Perkin Elmer), the diameter of cell clusters stained with calcein was analyzed using the longest axis measurement function in Volocity. Analysis with Volocity included use of the following functions: find objects, close, fill holes in objects, remove noise from objects, separate touching objects, and exclude objects by size (objects <1500 μm^3).

Immunostaining of cells in 3D culture. Hydrogels containing cells were rinsed with PBS (2 × 5 min, 37 °C) and then fixed with 4% paraformaldehyde (15 mins, room temperature). Gels were washed with PBS (1 × 5 min, room temperature), and then with a solution of 3% bovine serum albumin (BSA) and 0.05% Triton-X in PBS (2 × 5 min, room temperature). Cells were permeabilized and blocked by incubating with a solution of 5% BSA and 0.1% Triton-X in PBS (1 h, room temperature). Ki-67 samples were stained by incubating with solution of 2 μg mL^{-1} Anti-Ki-67 antibody (abcam), 5% BSA, and 0.1% Triton-X in PBS (4 °C, overnight). Gels were washed with a solution of 3% BSA and 0.05% Triton-X in PBS (3 × 30 mins, room temperature). Secondary antibody was added by incubating in a solution of goat anti-mouse AF647 (Invitrogen), phalloidinTRITC, 5% BSA, and 0.1% Triton-X in PBS (4 °C, overnight). Gels were washed with 3% BSA and 0.05% Triton-X in PBS (3 × 30 mins, room temperature). Gels were incubated with DAPI solution (700 nM DAPI in PBS, 1 h, room temperature). Gels were washed with PBS (3 × 30 mins, room temperature) and

imaged immediately with a LSM 810 confocal microscope (Zeiss). FIJI was use for image processing and quantification of Ki-67 positive cells.

3. RESULTS AND DISCUSSION

3.1 Design of nucleophilic thiol-yne PEG hydrogel-based ECM mimics

Click chemistries have shown great utility for the rapid formation of synthetic hydrogels for cell culture applications; yet, a need remains for materials chemistries free of catalyst and initiator that allow the formation of well-defined synthetic mimics of the ECM using accessible precursors. Thiol-yne chemistry offers an opportunity to easily create a versatile cell culture platform that provides control of chemical and mechanical properties with reaction conditions relevant for the encapsulation of the wide range of cells that may be sensitive to significant changes in temperature, pH, radicals *etc*. Towards establishing this cell culture platform for breast cancer cell culture, a range of PEG precursors with different architecture and molecular weights were functionalized with alkyne or thiol end groups (conversion >84%). As previously reported,[59] 3 arm (1 kg mol^{-1}) PEG alkyne was synthesized using propiolic acid through a simple Fischer esterification process. Thiol terminated PEG precursors were synthesized in a similar manner using 3-mercaptopropionic acid with 2 or 3 arm PEG precursors at 2 kg mol^{-1}, or 1 kg mol^{-1} respectively. Hydrogels were then formed at 10 wt% in either PBS (pH 7.4) or DMEM in a 1:1 alkyne:thiol ratio. As a consequence of the highly efficient nature of the thiol-yne reaction, no further purification steps were needed, and the hydrogels were used as prepared. Hydrogel nomenclature is dependent on the PEG precursors and peptide incorporation, each component is denoted considering the number of arms, molecular weight, and the incorporated functionality, **S** for thiol, **A** for alkyne or **P** for peptide. Hence, $\mathbf{3_{1S}}$ refers to the 3-arm thiol terminated PEG precursor (1 kg mol^{-1}) (Scheme 1).

Hydrogels, formed using this chemistry, degrade by ester hydrolysis over time, allowing for cell proliferation, which often is critical to long term cell culture in three dimensions. However, if degradation occurs too rapidly, the structural support will not be

maintained for the duration of the cell study. Here, we have selected the $\mathbf{3_{1A}3_{1S}}$ system, a high modulus network (*G'*= 10 kPa), to ensure the capability of prolonged cell culture, (10 days). This system has been shown to rapidly form robust materials which are stable for over 30 days, as a consequence of its slow degradation profile in aqueous environments.[59]

We have previously demonstrated the initial cyctocompatiblity of the nucleophilic thiol-yne PEG hydrogel $\mathbf{3_{1A}3_{1S}}$ system;[59] however, its design lacked the incorporation of either cell-degradable or cell adhesive peptides toward mimicking aspects of native cell-matrix interactions. Incorporating short receptor-binding peptides inspired by the insoluble proteins present in the native ECM allows the cells to interact with the synthetic network and can provide handles to maintain cell viability over long-term cell culture, promote cell proliferation, or mimic various extracellular environments.[52, 64] In particular, the vitronectin/fibronectin mimetic adhesion sequence, RGDS, has been incorporated into a variety of synthetic matrices to impart biological activity and has been previously shown to be relevant for promoting adhesion of breast cancer cells, including MCF-7s.[52, 64] Here, a thiol functionalized **C**GRGDS was thus selected for incorporation within thiol-yne synthetic matrices as an initial demonstration of the capability of this materials chemistry for incorporating receptor-binding ligands relevant for 3D culture, similar to previous demonstrations in thiol-ene hydrogel matrices.[65] The versatile nature of the thiol-yne hydrogel system allows for gelation even when the stoichiometry of the end groups (alkyne:thiol) deviates from 1:1. In fact, robust hydrogel networks can be synthesized with a large range of thiol end group concentrations (up to 20 mM less PEG thiol functionality, data not shown), supporting the potential to incorporate high concentrations of bioactive functionalities into the network. To allow for the peptide incorporation, the stoichiometry of thiol functional groups was reduced by 5 mM enabling available alkyne groups to react with the added 5 mM of RGDS while maintaining the stoichiometric ratio of overall thiol and

alkyne content within the system, $\mathbf{3_{1A}3_{1S}P_{RGDS}}$. This increased the gelation time of the system by reducing the number of crosslinking sites as the RGDS did not contribute to the overall gel formation. We were able to confirm that the pendant RGDS was covalently incorporated in the network throughout the cell study experiments by monitoring the fluorescence of hydrogels modified with a fluorescent RGDS ($\mathbf{3_{1A}3_{1S}P_{RGDS}}$ system), (Figure S2). The results demonstrate the successful incorporation of 1.8 mM peptide into the network upon the inclusion of 5 mM peptide at network formation. This concentration is comparable to other systems incorporating bioactive peptides, in which cell attachment and interaction with the matrix was observed.[66] This further highlights the thiol-yne hydrogels ability to mimic aspects of the ECM through the facile inclusion of ECM-inspired adhesion peptides. Note, RGDS alone previously has not be observed to significantly impact high-level responses of MCF7s in 3D culture (e.g., morphology, proliferation, invasion);[30] however, with our demonstration of successful peptide incorporation using RGDS, the impact of different ligands (or combinations of them) on cell function could be investigated in future studies with this thiol-yne 3D culture system.

In addition to imparted bioactivity, cells need to have space to grow and proliferate, which can be achieved in a number of ways (*e.g.*, matrix degradation or stress relaxation), ultimately allowing encapsulated cells to remodel their surroundings; indeed, this remodeling process has been shown to be a key feature in the application of synthetic materials as 3D cell culture scaffolds, particularly to allow for proliferation over time.[67-69] Control over degradability of gels can be obtained by either incorporating a thermally-responsive segment or by modifying the PEG architecture.[59] Although the $\mathbf{3_{1A}3_{1S}}$ system provides the desired stability for long-term cell culture, the limited degradability of the dense network over the observed culture time may prevent the proliferation and spreading of cells. Toward testing this, a di-thiol PEG precursor ($\mathbf{2_{2S}}$, 2 kg mol^{-1}) was incorporated into the $\mathbf{3_{1A}3_{1S}}$ and

$\mathbf{3_{1A}3_{1S}P_{RGDS}}$ networks to create two blended systems, $\mathbf{3_{1A}2_{2S}3_{1S}}$ and $\mathbf{3_{1A}2_{2S}3_{1S}P_{RGDS}}$, and tune the degradability of this system. In these blended systems, the thiol functional groups are mixed at a ratio of 10:90 $\mathbf{2_{2S}}$:$\mathbf{3_{1S}}$ (See SI for optimization of the PEG thiol ratio, Table S1). Furthermore, to increase the ability of cells to interact with their synthetic environment and increase degradability of the system, a matrix metalloproteinase (MMP) degradable di-thiol functionalized linker was incorporated into the network, ($\mathbf{3_{1A}2_{MMPS}3_{1S}}$) which allows the network to be locally degraded by the cells.[70] Similar to the above blended systems, the thiol functional groups were mixed at a ratio of 10:90 $\mathbf{2_{MMPS}}$:$\mathbf{3_{1S}}$. For the $\mathbf{3_{1A}2_{MMPS}3_{1S}}$ system, the MMP linker was incorporated into the system by substituting it for the PEG di-thiol precursor, as they have similar molecular weights (1.7 kg mol^{-1} and 2 kg mol^{-1} respectively). The $\mathbf{3_{1A}2_{MMPS}3_{1S}}$ system includes 5 mM RGDS similar to the $\mathbf{3_{1A}3_{1S}P_{RGDS}}$ and $\mathbf{3_{1A}2_{2S}3_{1S}P_{RGDS}}$ systems to increase cell interaction with the synthetic matrix and promote cell viability. For clarity the addition of $\mathbf{P_{RGDS}}$ has not been included in nomenclature for the $\mathbf{3_{1A}2_{MMPS}3_{1S}}$ system; however, RGDS has been incorporated throughout the testing of the $\mathbf{3_{1A}2_{MMPS}3_{1S}}$ system.

Overall, in this study, five different thiol-yne hydrogel networks have been synthesized ($\mathbf{3_{1A}3_{1S}}$, $\mathbf{3_{1A}3_{1S}P_{RGDS}}$, $\mathbf{3_{1A}2_{2S}3_{1S}}$, $\mathbf{3_{1A}2_{2S}3_{1S}P_{RGDS}}$ and $\mathbf{3_{1A}2_{MMPS}3_{1S}}$, Scheme 1), with the aim of creating synthetic extracellular matrices incorporating different peptide motifs and tuning their degradation profiles. Furthermore, these studies illustrate the importance that chemistry has in the synthesis of biomaterials, where careful design and selection of monomers was used to easily tune matrix properties with robust and accessible thiol-yne reaction, which ultimately will lead to their success in encapsulating and supporting the culture of cells.

3.2 Characterization of thiol-yne PEG hydrogels

Initial characterization of various network compositions was carried out through gelation time (vial tilt method) and swelling kinetic profile characterization. All the hydrogels

formed within 5 minutes in PBS; however, in DMEM, the networks formed much faster (less than 1 minute), (Table S2) as a consequence of the increased pH of the medium, increasing the rate of the nucleophilic thiol-yne addition reaction. While fast, this rate of gelation is similar to that observed with other chemistries used for the formation of step growth hydrogels used for cell encapsulation (e.g., SPAAC, thiol-maleimide).[25, 46]

The swelling profile of the materials varied greatly when the networks were formed off stoichiometry (alkyne:thiol groups deviate from 1:1), which is desirable for adding bioactive pendant peptides into the network structure (Figure 1a). As previously demonstrated, when formed in PBS, the $\mathbf{3_{1A}3_{1S}}$ system shrinks initially and then maintains a steady state for over 30 days.[59] However, when the network is formed with 5 mM less thiol end groups, this initial shrinking is prevented, and the swelling profile remains consistent for the duration of the 30-day experiment (Figure 1a), thus providing an unexpected advantage for cell encapsulation and culture. As expected, when the stoichiometry of the reactive groups changes (-5mM $\mathbf{3_{1S}}$), the density of the network decreased, thus allowing more water to be drawn into the network and enabling the system to swell, ultimately changing the swelling profile of the system. Moreover, the $\mathbf{3_{1A}3_{1S}P_{RGDS}}$ (addition of RGDS to the $\mathbf{3_{1A}3_{1S}}$-5mM system) gives an intermediate swelling profile, demonstrating the influence the peptide has on the swelling profile of the network. However, all systems visually resist degradation, with their robust structure maintained over 30 days.

When formed in serum-free medium in the presence of cells, the gelation time increased to several minutes allowing for the successful encapsulation of cells. Additionally, the initial shrinkage of $\mathbf{3_{1A}3_{1S}P_{RGDS}}$ is reduced compared to the original $\mathbf{3_{1A}3_{1S}}$ system, (Figure 1b) which is further observed when a di-thiol is also incorporated into the system, $\mathbf{3_{1A}2_{2S}3_{1S}P_{RGDS}}$, and the networks start to swell and degrade rapidly. This rapid degradation is a result of the presence of cells during the crosslinking reaction, disrupting the efficiency of

the reaction, reducing the density of the network formed. This in turn allows more water to infiltrate into the system and increases the rate of ester hydrolysis of the functional end groups, causing the hydrogels to degrade more rapidly. Nevertheless, the increase in swelling over the course of 3D cell culture gives rise to less dense pore structures, allowing for additional cell proliferation at later time points as detailed below.

Characterization of hydrogel stiffness was carried out through rheological and compression experiments, to understand the hydrogels' mechanical properties for the development of ECM mimics. Based on the rheological and compression data, thiol-yne PEG hydrogels synthesized in serum-free media allows the creation of environments ranging in stiffness from *G'*= 10 kPa for the original $\mathbf{3_{1A}3_{1S}}$ system to *G'*= 4 kPa for the $\mathbf{3_{1A}2_{2S}3_{1S}P_{RGDS}}$ system (Figure 1c and S3). Only the $\mathbf{3_{1A}2_{2S}3_{1S}P_{RGDS}}$ system was significantly different (ρ < 0.05) from the original $\mathbf{3_{1A}3_{1S}}$ system, as a result of the incorporation of a dithiol PEG precursor in addition to the pendant peptide incorporation. The stiffness of the materials decreased as the crosslinking density decreased: forming the hydrogels off stoichiometry reduced the number of crosslinked sites, reducing the rigidity of the hydrogel and therefore reducing *G'*. Furthermore, through the addition of a pendant hydrophilic peptide to the network, more water is drawn into the system, swelling the network and making a softer gel with a lower *G'*. However, the compressive strength of these materials is not affected by the change in stoichiometry of the end groups or by the addition of RGDS to the network (no significant difference ρ < 0.05), demonstrating the robust nature of nucleophilic thiol-yne addition to form hydrogels (Table S2 and Figure S3). The Young's moduli (*E*), calculated from $E = 2G(1 + \vartheta)$ where $G = \sqrt{G'^2 + G''^2}$ and ϑ = 0.5 (Poisson's ratio), for these materials ranges from 30.9 ± 0.4 kPa for $\mathbf{3_{1A}3_{1S}}$ to 13.4 ± 0.035 kPa for $\mathbf{3_{1A}2_{2S}3_{1S}P_{RGDS}}$, (Figure 1d and S3), mimicking the moduli of a range of soft tissues including different stages of breast cancer progression (*e.g.,* low to high grade infiltrating ductal carcinoma).[71, 72] As

observed in the rheological data, the only significantly difference in Young's modulus was for the $\mathbf{3_{1A}2_{2S}3_{1S}P_{RGDS}}$ system, as a result of the dithiol PEG precursor and the incorporation of RGDS decreasing the number of crosslinked sites in the network and therefore decreasing the modulus of the ECM scaffold.

3.3 2D cell culture of breast cancer cells in hydrogel formation-mimetic conditions

The use of cytocompatible chemistry is essential for the formation of 3D culture platforms that allow the encapsulation of cells within the network. As previous work has shown, the nucleophilic thiol-yne addition is biocompatible with a range of cell lines, highlighting the ideal characteristics it possesses as a crosslinking reaction for cell culture platforms.[55, 56, 58]Additionally, the lack of catalysts and free radicals during gel formation make it a potentially useful tool for encapsulation of sensitive cell lines. As an initial evaluation of the suitability of this chemistry for probing breast cancer cell growth, three different breast cancer cell lines were investigated: MDA-MB-231, a highly invasive, ER- breast cancer cell line; T47D, a ER+ breast cancer cell line; and MCF-7, an ER+ non-invasive tumorigenic breast cancer cell line. Non-gel forming thiol-yne reaction conditions were incubated with plated cells for each breast cancer cell line, using the commonly employed radically-initiated thiol-ene reaction as a comparison (Figure 2). Metabolic activity appears high for all conditions with the exception of the PEG alkyne condition, which showed dramatically low metabolic activity across all cell lines. These results highlight a key characteristic of the ester linked thiol-yne precursors. If the PEG alkyne precursor is presented to the cells in the absence of free thiols, thus preventing the thiol-yne reaction from occurring, the precursor is toxic. This is most likely a consequence of ester hydrolysis, which cleaves the ester bond very rapidly releasing propiolic acid (LD_{50} = 100 mg kg^{-1}) to the cells; indeed, cytotoxicity of propiolic acid in culture medium was confirmed, where significant decreases in metabolic activity were observed when cells were incubated with similar

concentrations to those used for hydrogel formation (Figure S4). In contrast, the metabolic activity is recovered in the thiol-yne condition, in which a stoichiometric amount of cysteine is presented to react with the available alkynes of the 3 arm PEG alkyne. The crosslinking product of the thiol-yne reaction, the thiolalkene, has increased stability to ester hydrolysis, and as a result, does not negatively influence cell proliferation.

There is a less dramatic, yet significant, reduction in metabolic activity of MCF-7 cells for the thiol-ene treatment, for which the MDA-MB-231 and T47D cell lines have shown no reduction in metabolic activity. This result suggests a sensitivity of MCF-7 cells to reaction conditions which utilize photoinitated free radicals during the crosslinking reaction. These results are consistent with previous preliminary data (data not shown) in which we have observed that the MCF-7 cells are sensitive to some mild photopolymerization conditions, in particular to free radical exposure during photoinitiation (10 mW cm^{-2} at 365 nm with lithium acylphosphinate [LAP] initiator). By day 3, the MCF-7 cells also show a metabolic activity that is statistically different ($\rho < 0.05$) from the growth medium control for the thiol-yne gel mimetic treatment, yet the metabolic activity remains high in comparison to the photoinitiated thiol-ene reaction condition mimic (86.7% and 63.5%, respectively, statistically different $\rho < 0.05$), suggesting that the thiol-yne reaction conditions may be more suitable for the encapsulation of MCF-7 cells. These initial 2D results highlight a potential benefit of using the nucleophilic thiol-yne addition as an alternative to the commonly used radically-initiated thiol-ene chemistry for hydrogel crosslinking in the presence of sensitive cell lines.

3.4 3D encapsulation of breast cancer cells in thiol-yne PEG hydrogels

In vitro synthetic cell culture platforms provide a well-controlled environment, which we can use to further understand the growth and behavior of breast cancer cells. An advantage for the use of bulk hydrogel materials as 3D cell culture platforms is that it is not

necessary for cells to migrate into the material after scaffold synthesis. However, by forming the 3D culture environment in the presence of cells, it is essential for the crosslinking chemistry to be cytocompatible. Therefore, after initial biocompatibility testing in 2D culture, we have explored the nucleophilic thiol-yne addition pathways as a route to encapsulate breast cancer cells for 3D culture.

Preliminary encapsulation experiments were carried out in the $\mathbf{3_{1A}3_{1S}}$ hydrogels formed in PBS. This system allowed for the successful encapsulation of MDA-MB-231 and T47D cell lines at early time points (day 1 and day 3, Figure 3), as shown by the high metabolic activity and cell viability. However, the metabolic activity of MCF-7 cells in this system was low, and live/dead images show very small cell bodies suggesting unhealthy or dying cells (Figure 3c). We hypothesized this to be a result of the sensitivity of the MCF-7 cells to PBS for extended times (Figure S5 and S6). Hence, to test this hypothesis that the observed cell death was a consequence of sensitivity to encapsulation conditions in PBS, we encapsulated MCF-7 cells in $\mathbf{3_{1A}3_{1S}P_{RGDS}}$ hydrogels synthesized in serum-free DMEM (Figure 4). When synthesizing these systems in DMEM in the presences of cells, the gelation time increased, allowing the solution to be easily pipetted into suitable molds for the formation of well-defined, homogenous cell-gel constructs for future testing. Cells were encapsulated evenly with the resulting hydrogels, as confirmed by 3D renderings of cell distributions within the gels (Figure S7). To demonstrate the mild nature of the nucleophilic thiol-yne addition chemistry, commonly utilized radically-initiated thiol-ene hydrogels were also synthesized in DMEM in the presence of MCF-7 cells. As the thiol-ene hydrogel system exhibits a very different swelling profile to the thiol-yne system (3.1 times more swelling), two seeding densities were also examined (2,500 cells μL^{-1} and 7,750 cells μL^{-1}). The lower seeding density contained the same total number of cells as the thiol-yne condition, and the higher seeding density replicated the same cell density in the materials after swelling, to

account for the potential effects of cell-cell interactions on cell proliferation. The thiol-ene chemistry led to significantly lower cell metabolic activity in comparison to the thiol-yne chemistry in all cases (Figure 4a). This is further confirmed through live/dead cell images, which show small cell bodies and punctate staining in the thiol-ene hydrogel system in comparison to the thiol-yne hydrogel system where the cells are much larger and uniformly brighter with few dead cells, (Figure 4b and c). These results further support our initial results in 2D culture studies that suggested the sensitivity MCF-7 cells have for otherwise gentle photopolymerization conditions. This result demonstrates the vast potential of the thiol-yne chemistry as a crosslinking reaction for the encapsulation of cell lines that are sensitive to the presence of free radicals.[37, 38, 54, 73] This hydrogel scaffold system provides a well-defined synthetic *in vitro* platform that enables the 3D encapsulation of MCF-7 cells, and potentially other sensitive cell lines, opening the door to future studies for better understanding of breast cancer progression and other processes in variety of tissue regeneration and disease applications.

3.5 MCF-7 cell proliferation in degradable ECM mimetic thiol-yne PEG hydrogels

Network degradability is one route to allow cells to grow and proliferate over time within hydrogel-based 3D cell culture platforms. As previously stated, one approach to increasing network degradability is the incorporation of di-thiol functionalized PEG (2 kg mol^{-1}) into the system, $\mathbf{3_{1A}2_{2S}3_{1S}P_{RGDS}}$. With the reduction of the 3-arm thiol precursor and the addition of the pendant adhesion peptide, the network becomes less stiff, as shown by the rheology data (decrease in *G'* from 10 kPa to 4 kPa), which indicates that the structure is less dense, with increased pore size enabling the system to swell. Increased water uptake results in increased hydrolysis of the network, allowing the cells to grow and proliferate, as evident by the significant increase in metabolic activity at later time points compared to the less degradable $\mathbf{3_{1A}3_{1S}P_{RGDS}}$ system ($\rho < 0.05$) (Figure 5a). In the $\mathbf{3_{1A}2_{2S}3_{1S}P_{RGDS}}$ system, each

time point also has a statistically significant increase in metabolic activity compared to the previous time point ($\rho < 0.05$), whereas metabolic activity in the $\mathbf{3_{1A}3_{1S}P_{RGDS}}$ system is only statistically different when comparing day 1 and the day 10 time points ($\rho < 0.05$). Confirmation was also obtained visually through live/dead images, where small cluster formation begins at the day 3 time point and continues to day 10, in which large clusters of cells are present compared to the smaller clusters formed at the later time points in the $\mathbf{3_{1A}3_{1S}P_{RGDS}}$ system (Figure 5b-d). Image analysis of cell cluster size quantitatively confirms these visual observations of increased cluster diameter over time (Figure S8). The morphology of the clusters in these images is characteristic of MCF-7 cells, and similar to that typically observed in naturally-derived hydrogel systems.[74]

Cluster growth over time further was supported through the incorporation of a cell degradable linker within the thiol-yne network, ($\mathbf{3_{1A}2_{MMPS}3_{1S}}$). Incorporation of a matrix metalloproteinase (MMP) degradable peptide crosslinker (G**C**RDVPMS↓MRGGDR**C**G) imparts local degradability of the network by MMPs secreted by the cells. The resulting hydrogel-based system therefore has two methods of degradation: 1) ester hydrolysis from the ester bonds in the functionalized PEG precursor components that allows for bulk degradation of the hydrogel over time and 2) enzymatic hydrolysis of an MMP degradable crosslink that allows cells to locally degrade the network. In these materials, by day 10, the cell metabolic activity was significantly increased compared to the $\mathbf{3_{1A}2_{2S}3_{1S}P_{RGDS}}$ system ($\rho < 0.05$), (Figure 5a) suggesting that the cells are degrading the matrix which leads to increased cell activity and potentially proliferation. Again, the metabolic activity at each time point was significantly increased compared to the previous time point ($\rho < 0.05$). The formation of cell clusters also was observed at later time points: similar cluster sizes were observed to those in $\mathbf{3_{1A}2_{2S}3_{1S}P_{RGDS}}$ degradable only by hydrolysis, whereas both $\mathbf{3_{1A}2}$ systems had statistically larger clusters than those in the less-degradable $\mathbf{3_{1A}3_{1S}P_{RGDS}}$ at late

times, further supporting the importance of matrix degradation over time for cell growth in these systems (Figure 5d and Figure S8).[75, 76] Forming MCF-7 cell clusters in a fully synthetic hydrogel system demonstrates the potential of this chemistry to form a tunable platform for controlled culture of MCF-7 cells, with relevance for the culture of a variety of other cell types. These synthetic hydrogels afford the opportunity to reduce batch-to-batch variability between samples and provide a 'blank slate' for manipulation of matrix properties in various ways depending on the application required.

The continual increase in metabolic activity over the 10-day experiment suggested that the cell clusters were forming due to proliferation, and not exclusively as a result of cell migration from a single cell encapsulation to clusters. To continue to probe the mechanism of cell cluster formation, MCF-7 cells encapsulated in thiol-yne $\mathbf{3_{1A}2_{2S}3_{1S}P_{RGDS}}$ hydrogels were immunostained for a proliferation marker, Ki-67 (Figure 6). Ki-67, shown here in magenta, indicates that cells are in the active phases of the cell cycle and is associated with proliferation. Image quantification indicates that 41 ± 6% of cells on day 1 and 59 ± 6% of cells on day 3 were Ki-67 positive, values which are not statistically different ($\rho > 0.05$). The presence of Ki-67 suggests that, at least in part, cell clusters are growing as cells divide. Overall, this system provides a platform for observing the proliferation of cell clusters and has potential to be adapted to probe questions of cell interactions with their culture environment.

4. CONCLUSIONS

Development of well-defined matrices as tools for 3D cell culture towards understanding disease progression and drug evaluation for breast cancer, among other diseases, has great potential to inform and advance current treatment methods. To do so, the chemistry behind the material must be capable of reliably producing controlled mechanical properties and presenting desired bioactive functionality in a predictable manner, while also encapsulating cells without impacting their viability. In this work, we have demonstrated the use of the nucleophilic thiol-yne addition to create synthetic PEG hydrogels with a range of hydrogel stiffness, the ability to easily incorporate bioactive peptide, and tunable network degradability by ester hydrolysis and cell-driven degradation to allow for cell proliferation for long-term 3D cell culture. With this system, we have demonstrated the ability to successfully encapsulate three breast cancer cell lines, MDA-MB-231, T47D and MCF-7. By highlighting the sensitivity of MCF-7 cells to radical-initiated thiol-ene crosslinking chemistry, this work has demonstrated the efficacy of network formation by nucleophilic thiol-yne chemistry in serum-free media as a potential alternative for other sensitive cell lines, clearly demonstrating the importance the chemistry behind new biomaterials has on their future success. Furthermore, we have created a system capable of bulk network degradability as well as local degradability mediated by MMP secretion by cells within the culture and have demonstrated the formation of stable MCF-7 cell clusters within 10 days of 3D culture. Immunostaining of the proliferation marker, Ki-67, in combination with metabolic activity data, suggests the observed cell clusters are formed primarily by proliferation. This study has highlighted the benefits of nucleophilic thiol-yne addition chemistry for the formation of a synthetic 3D culture platform for a sensitive breast cancer cell line, opening the door for future studies to design more complex network compositions and observe their effect on the cluster formation and behavior of a variety of breast cancer cell lines, including the MCF-7 cell line. We

envision this 3D cell culture platform being used broadly to study the impact of various controlled mechanical and biochemical compositions on the cell fate and behavior of sensitive cell lines, as well as present opportunities for translation *in vivo* for applications in cell delivery and tissue regeneration.

ACKNOWLEDGEMENTS

This work was supported by the RSC Research Mobility Grant awarded to L.J.M. to travel and study at the University of Delaware. The EPSRC are also thanked for the award of a DTP studentship to L.J.M. ERC are acknowledged for support to A.P. D. (grant number: 681559). This work also was supported by the Delaware COBRE program, with grants from the National Institute of General Medical Sciences – NIGMS (5 P20 GM104316 and 5 P30 GM110758) from the National Institutes of Health; a Susan G. Komen Foundation Career Catalyst Research Grant to A.M.K. (CCR16377327), and the National Science Foundation IGERT SBE2 program at the University of Delaware (fellowship to K.L.W.). The authors thank Prof. Wilfred Chen for use of the automated plate reader and Ms. Elisa Ovadia for training in confocal microscopy and for generously providing cysteine-modified peptide and thiol-ene gel precursors.

REFERENCES

1. Quail, D. F.; Joyce, J. A., Microenvironmental regulation of tumor progression and metastasis. Nat. Med. 2013, 19, 1423.

2. Thoma, C. R.; Zimmermann, M.; Agarkova, I.; Kelm, J. M.; Krek, W., 3D cell culture systems modeling tumor growth determinants in cancer target discovery. Adv. Drug Delivery Rev. 2014, 69-70, 29-41.

3. Sasai, Y., Next-Generation Regenerative Medicine: Organogenesis from Stem Cells in 3D Culture. Cell Stem Cell 2013, 12, (5), 520-530.

4. Antoni, D.; Burckel, H.; Josset, E.; Noel, G., Three-Dimensional Cell Culture: A Breakthrough in Vivo. Int. J. Mol. Sci. 2015, 16, (3), 5517.

5. Lee, G. Y.; Kenny, P. A.; Lee, E. H.; Bissell, M. J., Three-dimensional culture models of normal and malignant breast epithelial cells. Nat. Methods 2007, 4, (4), 359-365.

6. Barkan, D.; El Touny, L. H.; Michalowski, A. M.; Smith, J. A.; Chu, I.; Davis, A. S.; Webster, J. D.; Hoover, S.; Simpson, R. M.; Gauldie, J.; Green, J. E., Metastatic Growth from Dormant Cells Induced by a Col-I-Enriched Fibrotic Environment. Cancer Res 2010, 70, (14), 5706-5716.

7. Choi, S.; Coonrod, S.; Estroff, L.; Fischbach, C., Chemical and physical properties of carbonated hydroxyapatite affect breast cancer cell behavior. Acta Biomater. 2015, 24, 333-342.

8. Benton, G.; George, J.; Kleinman, H. K.; Arnaoutova, I. P., Advancing Science and Technology Via 3D Culture on Basement Membrane Matrix. J. Cell. Physiol. 2009, 221, (1), 18-25.

9. Baker, E. L.; Bonnecaze, R. T.; Zamao, M. H., Extracellular Matrix Stiffness and Architecture Govern Intracellular Rheology in Cancer. Biophys. J. 2009, 97, (4), 1013-1021.

10. Schedin, P.; Keely, P. J., Mammary Gland ECM Remodeling, Stiffness, and Mechanosignaling in Normal Development and Tumor Progression. Cold Spring Harbor Perspect. Biol 2011, 3, (1), a003228.

11. Alemany-Ribes, M.; Semino, C. E., Bioengineering 3D environments for cancer models. Adv. Drug Delivery Rev. 2014, 79-80, (Supplement C), 40-49.

12. Owen, S. C.; Shoichet, M. S., Design of three-dimensional biomimetic scaffolds. J. Biomed. Mater. Res., Part A 2010, 94A, (4), 1321-1331.

13. Rijal, G.; Li, W., 3D scaffolds in breast cancer research. Biomaterials 2016, 81, (Supplement C), 135-156.

14. Lutolf, M. P.; Blau, H. M., Artificial Stem Cell Niches. Adv. Mater. 2009, 21, (32-33), 3255-3268.

15. Gjorevski, N.; Nelson, C. M., Bidirectional extracellular matrix signaling during tissue morphogenesis. Cytokine Growth Factor Rev. 2009, 20, (5-6), 459-465.

16. Regier, M. C.; Montanez-Sauri, S. I.; Schwartz, M. P.; Murphy, W. L.; Beebe, D. J.; Sung, K. E., The Influence of Biomaterials on Cytokine Production in 3D Cultures. Biomacromolecules 2017, 18, (3), 709-718.

17. Trappmann, B.; Baker, B. M.; Polacheck, W. J.; Choi, C. K.; Burdick, J. A.; Chen, C. S., Matrix degradability controls multicellularity of 3D cell migration. Nat. Commun. 2017, 8, (1), 371.

18. Walters, N. J.; Gentleman, E., Evolving insights in cell–matrix interactions: Elucidating how non-soluble properties of the extracellular niche direct stem cell fate. Acta Biomater. 2015, 11, 3-16.

19. Caliari, S. R.; Burdick, J. A., A practical guide to hydrogels for cell culture. Nat. Methods 2016, 13, 405.

20. Baker, A. E. G.; Tam, R. Y.; Shoichet, M. S., Independently Tuning the Biochemical and Mechanical Properties of 3D Hyaluronan-Based Hydrogels with Oxime and Diels–Alder Chemistry to Culture Breast Cancer Spheroids. Biomacromolecules 2017, 18, (12), 4373-4384.

21. Watt, F. M.; Huck, W. T. S., Role of the extracellular matrix in regulating stem cell fate. Nat. Rev. Mol. Cell Biol. 2013, 14, 467.

22. Håkanson, M.; Kobel, S.; Lutolf, M. P.; Textor, M.; Cukierman, E.; Charnley, M., Controlled Breast Cancer Microarrays for the Deconvolution of Cellular Multilayering and Density Effects upon Drug Responses. PLOS ONE 2012, 7, (6), e40141.

23. Gencoglu, M. F.; Barney, L. E.; Hall, C. L.; Brooks, E. A.; Schwartz, A. D.; Corbett, D. C.; Stevens, K. R.; Peyton, S. R., Comparative Study of Multicellular Tumor Spheroid Formation Methods and Implications for Drug Screening. ACS Biomater. Sci. Eng. 2017.

24. John, C.; Xiaoshan, Y.; Trung Dung, N.; Aylin, A.; Victoria, R. Z.; Siyuan, Z.; Pinar, Z., 3D hydrogel-based microwell arrays as a tumor microenvironment model to study breast cancer growth. Biomed. Mater. 2017, 12, (2), 025009.

25. Brooks, E. A.; Jansen, L. E.; Gencoglu, M. F.; Yurkevicz, A. M.; Peyton, S. R., Complementary, Semiautomated Methods for Creating Multidimensional PEG-Based Biomaterials. ACS Biomater. Sci. Eng. 2018, 4, (2), 707-718.

26. Pradhan, S.; Clary, J. M.; Seliktar, D.; Lipke, E. A., A three-dimensional spheroidal cancer model based on PEG-fibrinogen hydrogel microspheres. Biomaterials 2017, 115, 141-154.

27. Jabbari, E.; Sarvestani, S. K.; Daneshian, L.; Moeinzadeh, S., Optimum 3D Matrix Stiffness for Maintenance of Cancer Stem Cells Is Dependent on Tissue Origin of Cancer Cells. PLOS ONE 2015, 10, (7), e0132377.

28. Beck, J. N.; Singh, A.; Rothenberg, A. R.; Elisseeff, J. H.; Ewald, A. J., The independent roles of mechanical, structural and adhesion characteristics of 3D hydrogels on the regulation of cancer invasion and dissemination. Biomaterials 2013, 34, (37), 9486-9495.

29. Roudsari, L. C.; Jeffs, S. E.; Witt, A. S.; Gill, B. J.; West, J. L., A 3D Poly(ethylene glycol)-based Tumor Angiogenesis Model to Study the Influence of Vascular Cells on Lung Tumor Cell Behavior. Sci. Rep. 2016, 6, 32726.

30. Taubenberger, A. V.; Bray, L. J.; Haller, B.; Shaposhnykov, A.; Binner, M.; Freudenberg, U.; Guck, J.; Werner, C., 3D extracellular matrix interactions modulate tumour cell growth, invasion and angiogenesis in engineered tumour microenvironments. Acta Biomater. 2016, 36, 73-85.

31. Chen, C. S., 3D Biomimetic Cultures: The Next Platform for Cell Biology. Trends Cell Biol. 2016, 26, (11), 798-800.

32. Kurokawa, Y. K.; George, S. C., Tissue engineering the cardiac microenvironment: Multicellular microphysiological systems for drug screening. Adv. Drug Delivery Rev. 2016, 96, 225-233.

33. Ki-Hwan, N.; Alec, S. T. S.; Saifullah, L.; Sunghoon, K.; Deok-Ho, K., Biomimetic 3D Tissue Models for Advanced High-Throughput Drug Screening. J. Lab. Autom. 2014, 20, (3), 201-215.

34. Esch, E. W.; Bahinski, A.; Huh, D., Organs-on-chips at the frontiers of drug discovery. Nat. Rev. Drug Discovery 2015, 14, 248.

35. Skardal, A.; Shupe, T.; Atala, A., Organoid-on-a-chip and body-on-a-chip systems for drug screening and disease modeling. Drug Discovery Today 2016, 21, (9), 1399-1411.

36. Bhise, N. S.; Ribas, J.; Manoharan, V.; Zhang, Y. S.; Polini, A.; Massa, S.; Dokmeci, M. R.; Khademhosseini, A., Organ-on-a-chip platforms for studying drug delivery systems. J. Controlled Release 2014, 190, 82-93.

37. Thorpe, G. W.; Fong, C. S.; Alic, N.; Higgins, V. J.; Dawes, I. W., Cells have distinct mechanisms to maintain protection against different reactive oxygen species: Oxidative-stress-response genes. Proc. Natl. Acad. Sci. U. S. A. 2004, 101, (17), 6564-6569.

38. Chen, X.; Song, M.; Zhang, B.; Zhang, Y., Reactive Oxygen Species Regulate T Cell Immune Response in the Tumor Microenvironment. Oxid. Med. Cell. Longevity 2016, 2016, 10.

39. Jeon, J. S.; Bersini, S.; Gilardi, M.; Dubini, G.; Charest, J. L.; Moretti, M.; Kamm, R. D., Human 3D vascularized organotypic microfluidic assays to study breast cancer cell extravasation. Proc. Natl. Acad. Sci. U. S. A. 2015, 112, (1), 214-219.

40. Seliktar, D., Designing Cell-Compatible Hydrogels for Biomedical Applications. Science 2012, 336, (6085), 1124-1128.

41. Azagarsamy, M. A.; Anseth, K. S., Bioorthogonal Click Chemistry: An Indispensable Tool to Create Multifaceted Cell Culture Scaffolds. ACS Macro Lett. 2013, 2, (1), 5-9.

42. Kharkar, P. M.; Kiick, K. L.; Kloxin, A. M., Designing degradable hydrogels for orthogonal control of cell microenvironments. Chem. Soc. Rev. 2013, 42, (17), 7335-7372.

43. Grover, G. N.; Lam, J.; Nguyen, T. H.; Segura, T.; Maynard, H. D., Biocompatible Hydrogels by Oxime Click Chemistry. Biomacromolecules 2012, 13, (10), 3013-3017.

44. Zhu, J. M., Bioactive modification of poly(ethylene glycol) hydrogels for tissue engineering. Biomaterials 2010, 31, (17), 4639-4656.

45. Silva, R.; Fabry, B.; Boccaccini, A. R., Fibrous protein-based hydrogels for cell encapsulation. Biomaterials 2014, 35, (25), 6727-6738.

46. DeForest, C. A.; Sims, E. A.; Anseth, K. S., Peptide-Functionalized Click Hydrogels with Independently Tunable Mechanics and Chemical Functionality for 3D Cell Culture. Chem. Mater. 2010, 22, (16), 4783-4790.

47. Alakpa, Enateri V.; Jayawarna, V.; Lampel, A.; Burgess, Karl V.; West, Christopher C.; Bakker, Sanne C. J.; Roy, S.; Javid, N.; Fleming, S.; Lamprou, Dimitris A.; Yang, J.; Miller, A.; Urquhart, Andrew J.; Frederix, Pim W. J. M.; Hunt, Neil T.; Péault, B.; Ulijn, Rein V.; Dalby, Matthew J., Tunable Supramolecular Hydrogels for Selection of Lineage-Guiding Metabolites in Stem Cell Cultures. Chem 2016, 1, (2), 298-319.

48. Lin, F.; Yu, J.; Tang, W.; Zheng, J.; Defante, A.; Guo, K.; Wesdemiotis, C.; Becker, M. L., Peptide-Functionalized Oxime Hydrogels with Tunable Mechanical Properties and Gelation Behavior. Biomacromolecules 2013, 14, (10), 3749-3758.

49. Gould, S. T.; Darling, N. J.; Anseth, K. S., Small peptide functionalized thiol–ene hydrogels as culture substrates for understanding valvular interstitial cell activation and de novo tissue deposition. Acta Biomater. 2012, 8, (9), 3201-3209.

50. Engler, A. J.; Sen, S.; Sweeney, H. L.; Discher, D. E., Matrix Elasticity Directs Stem Cell Lineage Specification. Cell 2006, 126, (4), 677-689.

51. Cavo, M.; Fato, M.; Peñuela, L.; Beltrame, F.; Raiteri, R.; Scaglione, S., Microenvironment complexity and matrix stiffness regulate breast cancer cell activity in a 3D in vitro model. Sci. Rep. 2016, 6, 35367.

52. Singh, S. P.; Schwartz, M. P.; Lee, J. Y.; Fairbanks, B. D.; Anseth, K. S., A peptide functionalized poly(ethylene glycol) (PEG) hydrogel for investigating the influence of biochemical and biophysical matrix properties on tumor cell migration. Biomater. Sci. 2014, 2, (7), 1024-1034.

53. Baskin, J. M.; Prescher, J. A.; Laughlin, S. T.; Agard, N. J.; Chang, P. V.; Miller, I. A.; Lo, A.; Codelli, J. A.; Bertozzi, C. R., Copper-free click chemistry for dynamic in vivo imaging. Proc. Natl. Acad. Sci. U. S. A. 2007, 104, (43), 16793-16797.

54. Xia, B.; Krutkramelis, K.; Oakey, J., Oxygen-Purged Microfluidic Device to Enhance Cell Viability in Photopolymerized PEG Hydrogel Microparticles. Biomacromolecules 2016, 17, (7), 2459-2465.

55. Truong, V. X.; Tsang, K. M.; Forsythe, J. S., Nonswelling Click-Cross-Linked Gelatin and PEG Hydrogels with Tunable Properties Using Pluronic Linkers. Biomacromolecules 2017, 18, (3), 757-766.

56. Truong, V. X.; Ablett, M. P.; Richardson, S. M.; Hoyland, J. A.; Dove, A. P., Simultaneous Orthogonal Dual-Click Approach to Tough, in-Situ-Forming Hydrogels for Cell Encapsulation. J. Am. Chem. Soc. 2015, 137, (4), 1618-1622.

57. Bell, C. A.; Yu, J.; Barker, I. A.; Truong, V. X.; Cao, Z.; Dobrinyin, A. V.; Becker, M. L.; Dove, A. P., Independent Control of Elastomer Properties through Stereocontrolled Synthesis. Angew. Chem. 2016, 128, (42), 13270-13274.

58. Macdougall, L. J.; Truong, V. X.; Dove, A. P., Efficient In Situ Nucleophilic Thiol-yne Click Chemistry for the Synthesis of Strong Hydrogel Materials with Tunable Properties. ACS Macro Lett. 2017, 6, 93-97.

59. Macdougall, L. J.; Pérez-Madrigal, M. M.; Arno, M. C.; Dove, A. P., Nonswelling Thiol–Yne Cross-Linked Hydrogel Materials as Cytocompatible Soft Tissue Scaffolds. Biomacromolecules 2017, DOI: 10.1021/acs.biomac.7b01204.

60. Wang, H.; Qian, J.; Zhang, Y.; Xu, W.; Xiao, J.; Suo, A., Growth of MCF-7 breast cancer cells and efficacy of anti-angiogenic agents in a hydroxyethyl chitosan/glycidyl methacrylate hydrogel. Cancer Cell Int. 2017, 17, 55.

61. Sawicki, L. A.; Kloxin, A. M., Design of thiol-ene photoclick hydrogels using facile techniques for cell culture applications. Biomater. Sci. 2014, 2, (11), 1612-1626.

62. Sawicki, L. A.; Kloxin, A. M., Light-mediated Formation and Patterning of Hydrogels for Cell Culture Applications. J. Visualized Exp. 2016, (115), 54462.

63. Chaudhuri, O.; Koshy, S. T.; Branco da Cunha, C.; Shin, J.-W.; Verbeke, C. S.; Allison, K. H.; Mooney, D. J., Extracellular matrix stiffness and composition jointly regulate the induction of malignant phenotypes in mammary epithelium. Nat. Mater. 2014, 13, 970.

64. Wang, S.; Cai, X.; Wang, L.; Li, J.; Li, Q.; Zuo, X.; Shi, J.; Huang, Q.; Fan, C., DNA orientation-specific adhesion and patterning of living mammalian cells on self-assembled DNA monolayers. Chem. Sci. 2016, 7, (4), 2722-2727.

65. Raza, A.; Ki, C. S.; Lin, C.-C., The influence of matrix properties on growth and morphogenesis of human pancreatic ductal epithelial cells in 3D. Biomaterials 2013, 34, (21), 5117-5127.

66. Salinas, C. N.; Anseth, K. S., The influence of the RGD peptide motif and its contextual presentation in PEG gels on human mesenchymal stem cell viability. J. Tissue Eng. Regener. Med. 2008, 2, (5), 296-304.

67. Gong, Z.; Szczesny, S. E.; Caliari, S. R.; Charrier, E. E.; Chaudhuri, O.; Cao, X.; Lin, Y.; Mauck, R. L.; Janmey, P. A.; Burdick, J. A.; Shenoy, V. B., Matching material and cellular timescales maximizes cell spreading on viscoelastic substrates. Proc. Natl. Acad. Sci. U. S. A. 2018.

68. Chaudhuri, O.; Gu, L.; Klumpers, D.; Darnell, M.; Bencherif, S. A.; Weaver, J. C.; Huebsch, N.; Lee, H.-p.; Lippens, E.; Duda, G. N.; Mooney, D. J., Hydrogels with tunable stress relaxation regulate stem cell fate and activity. Nat. Mater. 2015, 15, 326.

69. Khetan, S.; Guvendiren, M.; Legant, W. R.; Cohen, D. M.; Chen, C. S.; Burdick, J. A., Degradation-mediated cellular traction directs stem cell fate in covalently crosslinked three-dimensional hydrogels. Nat. Mater. 2013, 12, (5), 458-465.

70. Schultz, K. M.; Kyburz, K. A.; Anseth, K. S., Measuring dynamic cell–material interactions and remodeling during 3D human mesenchymal stem cell migration in hydrogels. Proc. Natl. Acad. Sci. U. S. A. 2015, 112, (29), E3757-E3764.

71. Rehmann, M. S.; Kloxin, A. M., Tunable and dynamic soft materials for three-dimensional cell culture. Soft Matter 2013, 9, (29), 6737-6746.

72. Price, B. D.; Gibson, A. P.; Tan, L. T.; Royle, G. J., An elastically compressible phantom material with mechanical and x-ray attenuation properties equivalent to breast tissue. Phys. Med. Biol. 2010, 55, (4), 1177.

73. Belikov, A. V.; Schraven, B.; Simeoni, L., T cells and reactive oxygen species. J. Biomed. Sci. 2015, 22, 85.

74. Vantangoli, M. M.; Madnick, S. J.; Huse, S. M.; Weston, P.; Boekelheide, K., MCF-7 Human Breast Cancer Cells Form Differentiated Microtissues in Scaffold-Free Hydrogels. PLOS ONE 2015, 10, (8), e0135426.

75. Peela, N.; Sam, F. S.; Christenson, W.; Truong, D.; Watson, A. W.; Mouneimne, G.; Ros, R.; Nikkhah, M., A three dimensional micropatterned tumor model for breast cancer cell migration studies. Biomaterials 2016, 81, (Supplement C), 72-83.

76. Bray, L. J.; Binner, M.; Holzheu, A.; Friedrichs, J.; Freudenberg, U.; Hutmacher, D. W.; Werner, C., Multi-parametric hydrogels support 3D in vitro bioengineered microenvironment models of tumour angiogenesis. Biomaterials 2015, 53, (Supplement C), 609-620.

Scheme 1: Hydrogel formation: (a) Nucleophilic thiol-yne addition, (b) Legend for the alkyne, thiol and thiolalkene functionality, (c) Alkyne and thiol functionalised PEG architecture, (d) Hydrogel networks formed by thiol-yne chemistry at 10 wt%. Thiol and alkyne end group react upon mixing under basic conditions. Alkyne:Thiol ratio = 1:1 $\mathbf{3_{1A}3_{1S}}$ = 3-arm PEG alkyne ($\mathbf{3_{1A}}$) reacted with 3 arm PEG thiol ($\mathbf{3_{1S}}$), $\mathbf{3_{1A}2_{2S}3_{1S}}$ = $\mathbf{3_{1A}}$ reacted with a mixture of $\mathbf{3_{1S}}$ and 2-arm PEG thiol ($\mathbf{2_{2S}}$) in a ratio of 10:90, to increase the rate of hydrogel degradation, (e) Thiol functional bioactive peptide ($\mathbf{P_{RGDS}}$) and di-thiol functional cell degradable peptide ($\mathbf{2_{MMPS}}$), incorporated into the hydrogel network to enable cell adhesion and some cell-driven remodelling increase ECM characteristics, (f) Hydrogel network formation with bioactive peptides at 10 wt%. $\mathbf{2_{MMPS}}$ replaced $\mathbf{2_{2S}}$ in $\mathbf{3_{1A}2_{MMPS}3_{1S}}$. Note that all $\mathbf{3_{1A}2_{MMPS}3_{1S}}$ hydrogels also contain bioactive pendant peptide, however $\mathbf{P_{RGDS}}$ is not incorporated into the nomenclature.

Figure 1: (a) Swelling characteristics of the thiol-yne hydrogels synthesized in PBS; Comparison of $\mathbf{3_{1A}3_{1S}}$ (square) (1:1 alkyne:thiol end groups), $\mathbf{3_{1A}3_{1S}}$**-5mM** with reduced amount of $\mathbf{3_{1S}}$ (-5 mM) (circle), and $\mathbf{3_{1A}3_{1S}}$ $\mathbf{P_{RGDS}}$ (triangle). (b) Comparison of the swelling characteristics of the thiol-yne hydrogels made in serum-free DMEM with the encapsulation of MCF-7 cells over 1 week; $\mathbf{3_{1A}3_{1S}P_{RGDS}}$ (open circle), $\mathbf{3_{1A}2_{2S}3_{1S}P_{RGDS}}$ (cross), $\mathbf{3_{1A}2_{MMP}3_{1S}}$, 10:90 ratio of $\mathbf{2_{MMP}}$:$\mathbf{3_{1S}}$ (diamond). (c) Rheological properties of the thiol-yne hydrogels synthesised in serum-free DMEM. *G'* = Average storage modulus at a constant frequency of 10 rad s^{-1} and 0.5% strain. *G'* ranges from 10242 ± 1595 Pa for $\mathbf{3_{1A}3_{1S}}$ to 4461 ± 115 Pa for $\mathbf{3_{1A}2_{2S}3_{1S}P_{RGDS}}$ reflecting the addition of the RGDS peptide to the network. (d) Young's Modulus (E) calculated from $E = 2G(1 + \vartheta)$ where $G = \sqrt{G'^2 + G''^2}$ and ϑ = 0.5 (Poisson's ratio). Young's Modulus also reduces with the incorporation of RGDS from 30.9 ± 0.4 kPa for $\mathbf{3_{1A}3_{1S}}$ to 13.4 ± 0.035 kPa for $\mathbf{3_{1A}2_{2S}3_{1S}P_{RGDS}}$. α = Significantly different from $\mathbf{3_{1A}3_{1S}}$ conditions, $\rho < 0.05$.

Figure 2: Metabolic activity of breast cancer cells in 2D hydrogel formation-mimetic environments. Cells from three different breast cancer cell lines (MDA-MB-231, T47D and MCF-7) were seeded onto 96-well plates at a density of 15,000 cells cm^{-2}. After 24h of culture, cells were exposed to various hydrogel formation-mimetic conditions. Cells were exposed to all conditions for 15 mins, with the exception of the photo-initiated thiol-ene condition (2 min) to mimic reaction conditions. Day 1 indicates 24h after treatment with conditions. Metabolic assay was assessed by Cell-Titer 96 assay (Absorbance = 490 nm). (a) At day 1, cells exposed to the PEG alkyne in solution had a significantly lower metabolic activity than in all other conditions for all cell lines. T47D and MCF-7 cells had significantly higher metabolic activities than the growth medium control after exposure to the thiol-yne condition, (b) By day 3, only the PEG alkyne condition is different from the control for the MDA-MB-231 and T47D cells. However, the MCF-7 cells have a significant reduction across multiple conditions including PBS, thiol-yne, and most significantly, thiol-ene. α = Significantly different from control conditions, $\rho < 0.05$.

Figure 3: The metabolic activity of (a) MDA-MB-231 and T47D (5,000 cells μL^{-1}), and MCF-7 cells, (2,500 cells μL^{-1}), encapsulated in the $\mathbf{3_{1A}3_{1S}}$ (no RGDS) system formed in PBS solution (pH 7.4). Cell metabolic activity was assessed after 1 and 3 days of culture within the hydrogels by an alamarBlue assay. Fluorescence was measured on a plate reader (Ex = 560, Em = 590). (b) Live/Dead images of MDA-MB-231 cells encapsulated in $\mathbf{3_{1A}3_{1S}}$ hydrogels (5,000 cells μL^{-1}). (c) Live/Dead images of MCF-7 cells encapsulated in $\mathbf{3_{1A}3_{1S}}$ hydrogels (2,500 cells μL^{-1}). Live cells stained green (Calcein, Ex. = 495 nm, Em. = 515 nm), dead cells stained red (Ethidium homodimer, Ex = 528 nm, Em = 617 nm). Scale bar = 100 μm. These data suggest a sensitivity of the MCF-7 cells to the encapsulation conditions.

Figure 4: Encapsulation of MCF-7 cells in photo-initiated thiol-ene and thiol-yne ($\mathbf{3_{1A}3_{1S}P_{RGDS}}$) hydrogels formed in serum-free medium. Cells were encapsulated in the thiol-ene gels at two different cell concentrations (2,500 and 7,750 cells μL^{-1}). The former cell concentration is the same concentration used to encapsulate cells in the thiol-yne gels, and the later concentration accounts for the differences in swelling between the different gel compositions to provide a control for effects of cell-cell interactions. (a) MCF-7 cell metabolic activity was assessed after 1 and 3 days of culture within the hydrogels by an alamarBlue assay. Fluorescence was measured on a plate reader (Ex = 560, Em = 590). (b and c) Live/Dead images from Day 3 time point, live cells stained green (Calcein, Ex. = 495 nm, Em. = 515 nm), dead cells stained red (Ethidium homodimer, Ex = 528 nm, Em = 617 nm). (b) Thiol-ene condition (7,750 cells μL^{-1}), (c) thiol-yne condition (2,500 cells μL^{-1}). Scale bar = 50 μm. These data suggest that the thiol-yne hydrogel system provides a gentle cell encapsulation environment that is suitable for 3D encapsulation and culture of MCF-7 cells.

Figure 5: 3D culture of MCF-7 cells in degradable thiol-yne hydrogels. MCF-7 cells were encapsulated in various compositions of thiol-yne gels in serum-free medium (2,500 cells μL^{-1}). (a) The metabolic activity of MCF-7 cells in thiol-yne hydrogels was assessed by the alamarBlue assay at 1, 3, 7 and 10 days after encapsulation. Fluorescence was measured on a plate reader (Ex = 560, Em = 590). α = Significantly different values for day 10 between all gelation conditions, $\rho < 0.05$. Within the $\mathbf{3_{1A}2_{2S}3_{1S}P_{RGDS}}$ and $\mathbf{3_{1A}2_{MMPS}3_{1S}P_{RGDS}}$ conditions, the metabolic activity at each day is statistically different ($\rho < 0.05$) from the previous time point. For the $\mathbf{3_{1A}3_{1S}P_{RGDS}}$ condition, only the day 10 metabolic activity is statistically different ($\rho < 0.05$) from day 1. (b-d) Live/Dead imaging of the MCF-7 cells. Live cells stained green (Calcein, Ex. = 495 nm, Em. = 515 nm), dead cells stained red (Ethidium homodimer, Ex = 528 nm, Em = 617 nm). (b) $\mathbf{3_{1A}3_{1S}P_{RGDS}}$, (c) $\mathbf{3_{1A}2_{2S}3_{1S}P_{RGDS}}$ and (d) $\mathbf{3_{1A}2_{MMPS}3_{1S}P_{RGDS}}$. Scale bar = 50 μm. The incorporation of $\mathbf{2_{2S}}$ and $\mathbf{2_{MMPS}}$ significantly increased the metabolic activity by day 7 compared to the $\mathbf{3_{1A}3_{1S}P_{RGDS}}$ condition as well as the increased cluster formation. By day 10, the metabolic activity is significantly greater for the condition including the cell degradable crosslinker. This observation suggests, that the cells ability to locally degrade the matrix increases cell proliferation in these matrices.

Figure 6: Proliferation of MCF-7 cells in 3D cell culture. MCF-7 cells were encapsulated in $\mathbf{3_{1A}2_{2S}3_{1S}P_{RGDS}}$ hydrogels and immunostained for nuclei (blue), f-actin (red), and Ki-67 (magenta) 1 and 3 days after encapsulation. (a) Image quantification shows that 41 ± 6% of

cells on Day 1 and 59 ± 6% of cells on D3 were Ki-67 positive. These values are not statistically different ($\rho > 0.05$). (b) Representative images shown for day 1 time point. Scale bar = 50 μm. **(**c) Enlarged image to highlight Ki-67 positive cells. Scale bar = 25 μm. These data suggest that cell proliferation contributes to the observed cell cluster formation.

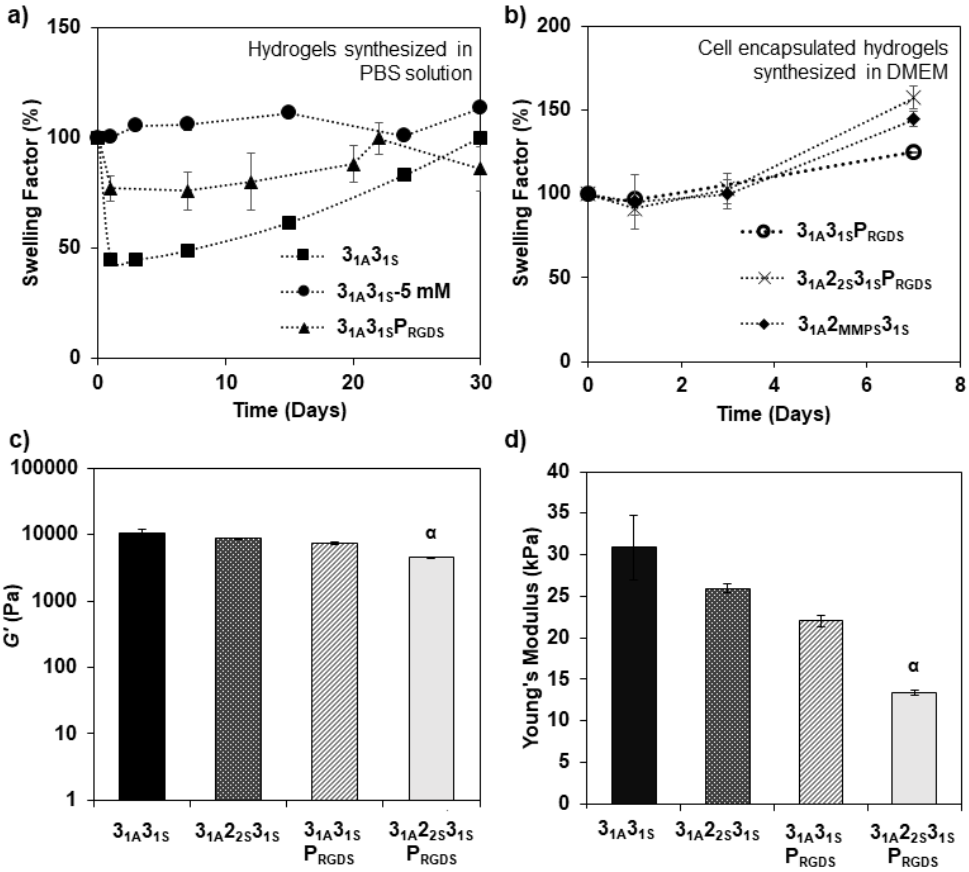
a)
Hydrogels synthesized in PBS solution
Swelling Factor (%)
Time (Days)
$3_{1A}3_{1S}$
$3_{1A}3_{1S}$-5 mM
$3_{1A}3_{1S}P_{RGDS}$
b)
Cell encapsulated hydrogels synthesized in DMEM
Swelling Factor (%)
Time (Days)
$3_{1A}3_{1S}P_{RGDS}$
$3_{1A}2_{2S}3_{1S}P_{RGDS}$
$3_{1A}2_{MMPS}3_{1S}$
c)
G' (Pa)
α
$3_{1A}3_{1S}$
$3_{1A}2_{2S}3_{1S}$
$3_{1A}3_{1S}$ P_{RGDS}
$3_{1A}2_{2S}3_{1S}$ P_{RGDS}
d)
Young's Modulus (kPa)
α
$3_{1A}3_{1S}$
$3_{1A}2_{2S}3_{1S}$
$3_{1A}3_{1S}$ P_{RGDS}
$3_{1A}2_{2S}3_{1S}$ P_{RGDS}

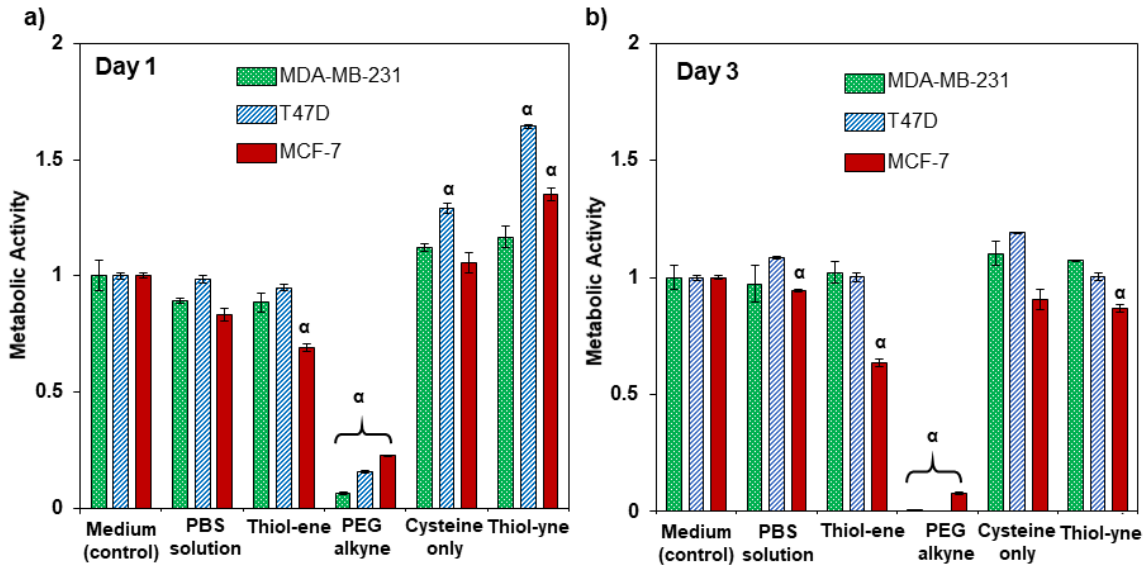
a)
Day 1
MDA-MB-231
T47D
MCF-7
Metabolic Activity
2
1.5
1
0.5
0
α
Medium (control)
PBS solution
Thiol-ene
PEG alkyne
Cysteine only
Thiol-yne
b)
Day 3
MDA-MB-231
T47D
MCF-7
Metabolic Activity
Medium (control)
PBS solution
Thiol-ene
PEG alkyne
Cysteine only
Thiol-yne

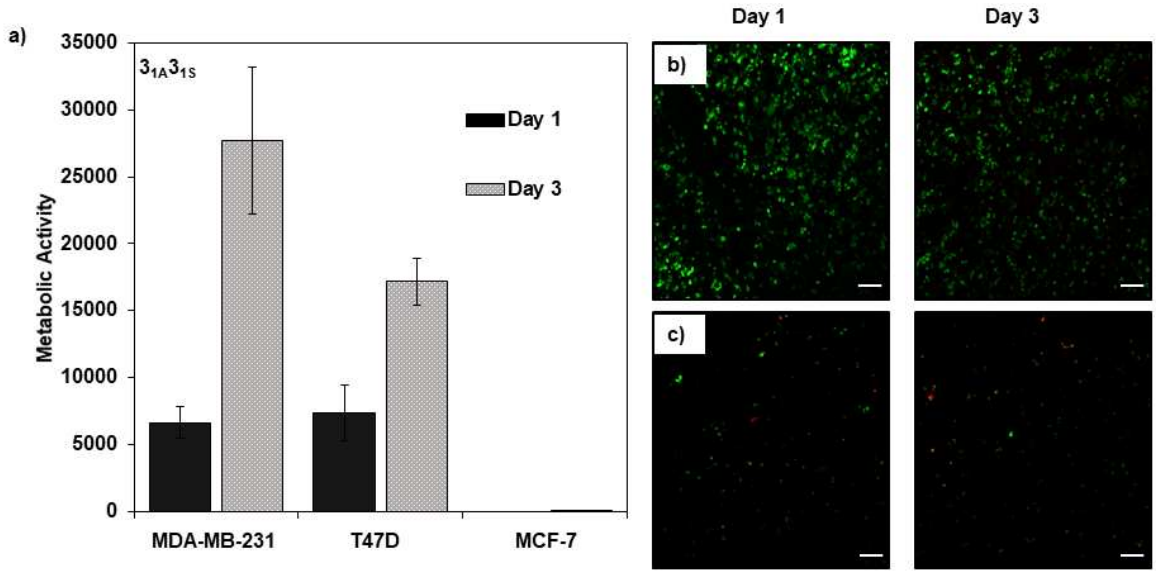
a)
$3_{1A}3_{1S}$
Metabolic Activity
35000
30000
25000
20000
15000
10000
5000
0
Day 1
Day 3
MDA-MB-231
T47D
MCF-7
Day 1
Day 3
b)
c)

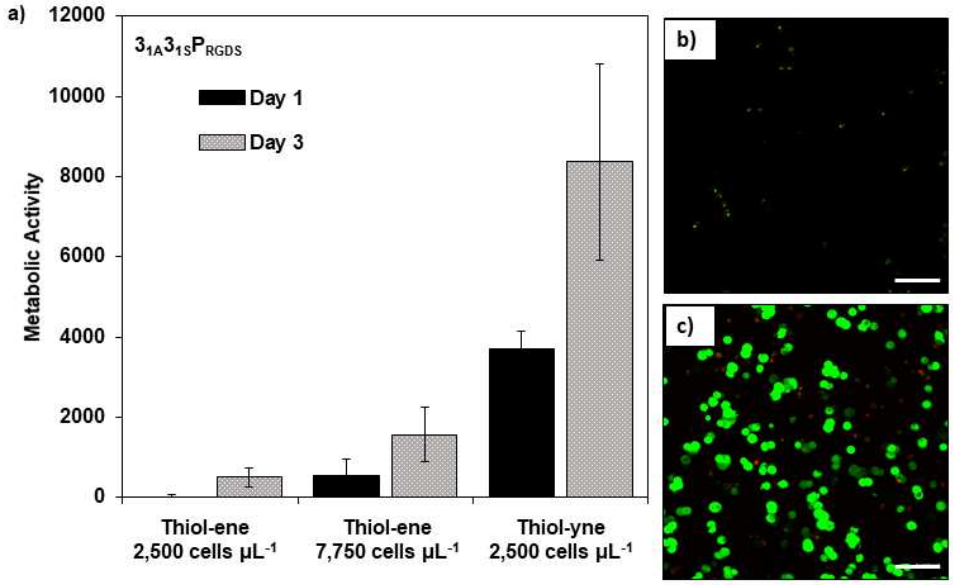
a)
12000
10000
8000
6000
4000
2000
0
$3_{1A}3_{1S}P_{RGDS}$
Day 1
Day 3
Metabolic Activity
Thiol-ene
2,500 cells µL-1
Thiol-ene
7,750 cells µL-1
Thiol-yne
2,500 cells µL-1
b)
c)

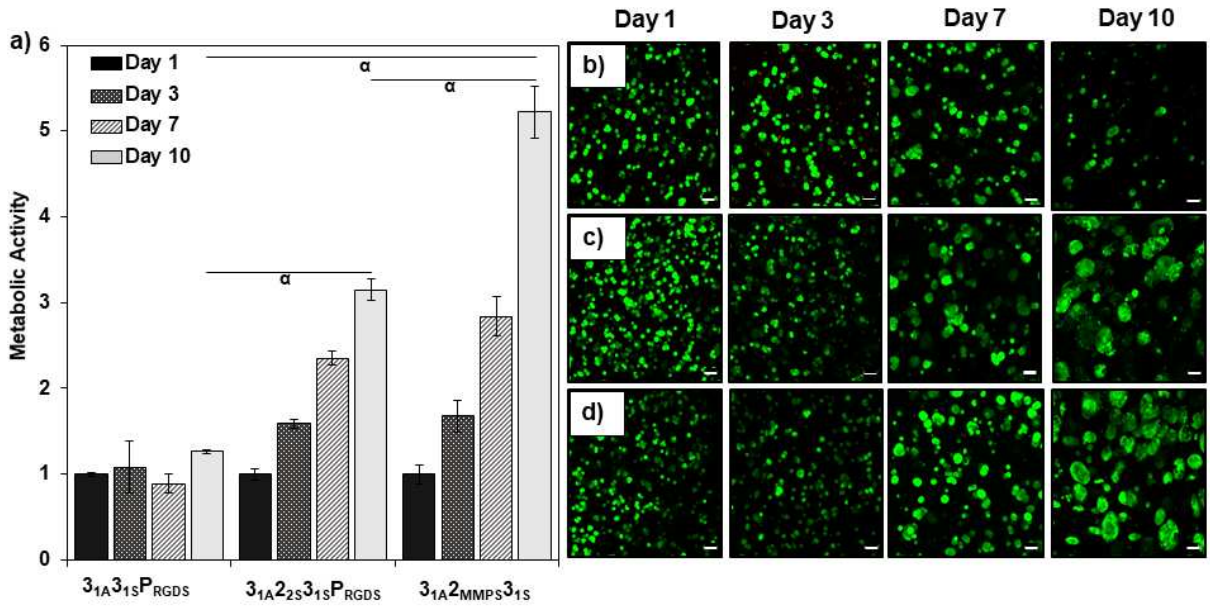
a)
Metabolic Activity
Day 1
Day 3
Day 7
Day 10
α
α
α
$3_{1A}3_{1S}P_{RGDS}$
$3_{1A}2_{2S}3_{1S}P_{RGDS}$
$3_{1A}2_{MMPS}3_{1S}$
Day 1
Day 3
Day 7
Day 10
b)
c)
d)

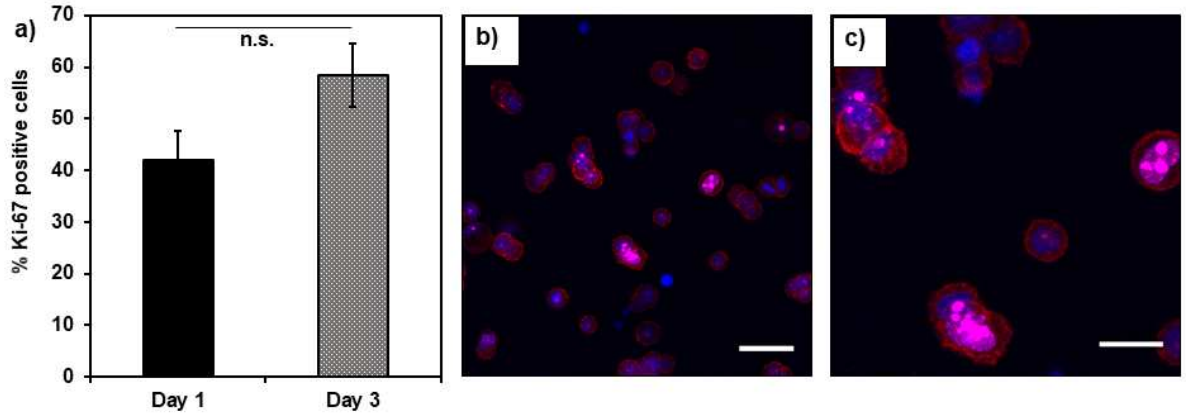

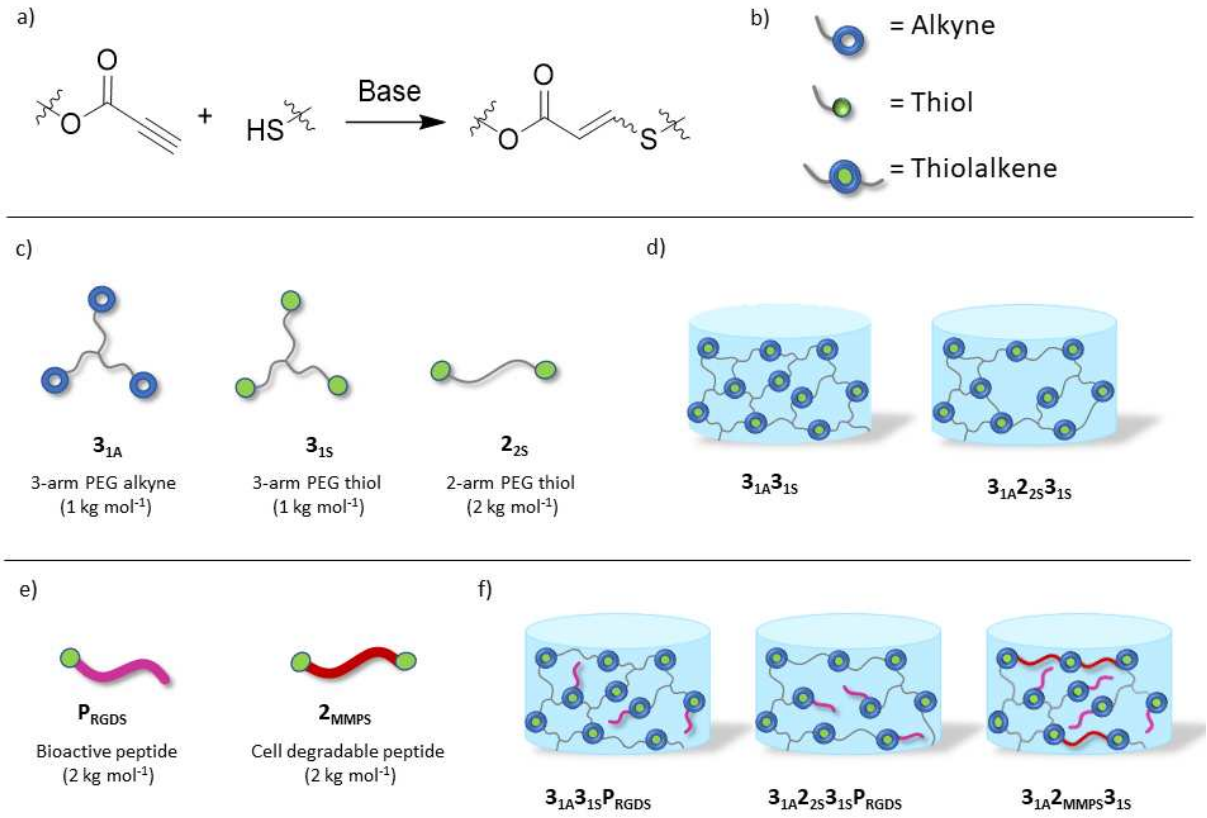
a)
Base
b)
= Alkyne
= Thiol
= Thiolalkene
c)
3_{1A}
3-arm PEG alkyne
(1 kg mol^{-1})
3_{1S}
3-arm PEG thiol
(1 kg mol^{-1})
2_{2S}
2-arm PEG thiol
(2 kg mol^{-1})
d)
$3_{1A}3_{1S}$
$3_{1A}2_{2S}3_{1S}$
e)
P_{RGDS}
Bioactive peptide
(2 kg mol^{-1})
2_{MMPS}
Cell degradable peptide
(2 kg mol^{-1})
f)
$3_{1A}3_{1S}P_{RGDS}$
$3_{1A}2_{2S}3_{1S}P_{RGDS}$
$3_{1A}2_{MMPS}3_{1S}$